AMERICAN JOURNAL OF PHYSIOLOGY
GASTROINTESTINAL AND LIVER PHYSIOLOGY

Am J Physiol Gastrointest Liver Physiol 324: G305–G321, 2023.
First published February 7, 2023; doi:10.1152/ajpgi.00231.2022

RESEARCH ARTICLE

Diet-induced obesity alters intestinal monocyte-derived and tissue-resident macrophages and increases intestinal permeability in female mice independent of tumor necrosis factor

Jessica A. Breznik,[1,2,3] Jennifer Jury,[4,5] Elena F. Verdú,[4,5] Deborah M. Sloboda,[4,5,6,7] and Dawn M. E. Bowdish[1,2,3]

[1]*McMaster Immunology Research Centre, McMaster University, Hamilton, Ontario, Canada;* [2]*Michael G. DeGroote Institute for Infectious Disease Research, McMaster University, Hamilton, Ontario, Canada;* [3]*Department of Medicine, McMaster University, Hamilton, Ontario, Canada;* [4]*Department of Biochemistry and Biomedical Sciences, McMaster University, Hamilton, Ontario, Canada;* [5]*Farncombe Family Digestive Health Research Institute, McMaster University, Hamilton, Ontario, Canada;* [6]*Department of Obstetrics and Gynecology, McMaster University, Hamilton, Ontario, Canada; and* [7]*Department of Pediatrics, McMaster University, Hamilton, Ontario, Canada*

Abstract

Macrophages are essential for homeostatic maintenance of the anti-inflammatory and tolerogenic intestinal environment, yet monocyte-derived macrophages can promote local inflammation. Proinflammatory macrophage accumulation within the intestines may contribute to the development of systemic chronic inflammation and immunometabolic dysfunction in obesity. Using a model of high-fat diet-induced obesity in C57BL/6J female mice, we assessed intestinal paracellular permeability by in vivo and ex vivo assays and quantitated intestinal macrophages in ileum and colon tissues by multicolor flow cytometry after short (6 wk), intermediate (12 wk), and prolonged (18 wk) diet allocation. We characterized monocyte-derived $CD4^{-}TIM4^{-}$ and $CD4^{+}TIM4^{-}$ macrophages, as well as tissue-resident $CD4^{+}TIM4^{+}$ macrophages. Diet-induced obesity had tissue- and time-dependent effects on intestinal permeability, as well as monocyte and macrophage numbers, surface marker phenotype, and intracellular production of the cytokines IL-10 and tumor necrosis factor (TNF). We found that obese mice had increased paracellular permeability, in particular within the ileum, but this did not elicit recruitment of monocytes nor a local proinflammatory response by monocyte-derived or tissue-resident macrophages in either the ileum or colon. Proliferation of monocyte-derived and tissue-resident macrophages was also unchanged. Wild-type and $TNF^{-/-}$ littermate mice had similar intestinal permeability and macrophage population characteristics in response to diet-induced obesity. These data are unique from reported effects of diet-induced obesity on macrophages in metabolic tissues, as well as outcomes of acute inflammation within the intestines. These experiments also collectively indicate that TNF does not mediate effects of diet-induced obesity on paracellular permeability or intestinal monocyte-derived and tissue-resident intestinal macrophages in young female mice.

NEW & NOTEWORTHY We found that diet-induced obesity in female mice has tissue- and time-dependent effects on intestinal paracellular permeability as well as monocyte-derived and tissue-resident macrophage numbers, surface marker phenotype, and intracellular production of the cytokines IL-10 and TNF. These changes were not mediated by TNF.

female; intestinal macrophages; intestinal permeability; obesity; tumor necrosis factor

INTRODUCTION

Macrophages are innate immune cells with diverse tissue-specific roles in maintenance of homeostasis (1) and in the initiation and resolution of the acute inflammatory response (2). Macrophages also contribute to the pathophysiology of chronic inflammatory diseases such as obesity (3). Like most tissues, the intestines contain a significant proportion of long-lived tissue-resident macrophages, as well as macrophages derived from blood monocytes, which originate from bone marrow progenitors (4–6). Macrophages are present along the entire length and within all structural layers of the intestines (5, 7, 8). Monocyte-derived macrophages are located proximal to the intestinal epithelium where they mediate interactions between the microbiota, luminal antigens, and other immune cells, to maintain epithelial barrier function, and ultimately support immunological tolerance and host defense (4, 5). Long-lived tissue-resident macrophages, in contrast, localize in the submucosal and muscularis layers of the intestinal wall and support the functions of blood and lymphatic vessels, enteric neurons, and smooth muscle cells (4, 5, 9). Monocyte-derived and tissue-resident

Correspondence: D. M. E. Bowdish (bowdish@mcmaster.ca).
Submitted 30 September 2022 / Revised 2 February 2023 / Accepted 5 February 2023

intestinal macrophages accordingly have distinct responses to inflammation.

Acute intestinal inflammation, as observed in infection, colitis, and after sterile injury, is often accompanied by rapid recruitment of bone marrow-derived Ly6C^{high} monocytes, which develop into immature proinflammatory macrophages that contribute to damage of the intestinal epithelial barrier (10–12). In contrast, tissue-resident macrophages maintain their anti-inflammatory phenotype and functions, preventing tissue injury from inflammation-elicited immune cells (11, 13, 14). Changes to monocyte-derived macrophage phenotype and function may also occur within intestinal tissues under conditions of the low-grade and chronic systemic inflammation that is characteristic of obesity (15). Obesity increases circulating Ly6C^{high} monocytes (16, 17), which differentiate into proinflammatory macrophages within metabolic tissues like adipose (18, 19). Although it has been reported that there is an accumulation of proinflammatory macrophages within the colon in obesity (20), which could contribute to observations of obesity-associated increases in gut permeability (20–23), there is a lack of consensus across published research (21, 24–27). This is likely due to differences in the methods and tissue regions of assessment, length of diet allocation, and selection of appropriate surface antigens to identify macrophages as well as to distinguish their monocyte-derived or tissue-resident phenotypes and functions. Importantly, it is also unclear which upstream driver(s) in obesity may contribute to changes in intestinal macrophages.

One such driver may be the proinflammatory cytokine tumor necrosis factor (TNF). Within the intestines, TNF is constitutively produced at low levels by intestinal epithelial enterocytes, stromal cells, macrophages, and other immune cells (28, 29). TNF regulates monocyte and macrophage survival and function (30), as well as homeostatic maintenance and repair of the intestinal epithelium (28). However, macrophage overproduction of TNF promotes intestinal inflammation in mouse models of colitis (31, 32), and in inflammatory bowel disease in humans (33, 34). Elevated levels of TNF can also mediate disruption of the intestinal barrier (28, 29). TNF has in addition been reported to contribute to chronic intestinal inflammation in obesity (20, 35–37). Recruitment of monocytes that differentiate into TNF-producing proinflammatory macrophages within intestinal tissues may therefore promote loss of barrier function that contributes to local inflammation as well as systemic immunometabolic dysfunction in obesity (20, 25).

In this study, we used a high-fat diet model in littermate wild-type and TNF knockout female mice to examine effects of obesity and the role of TNF within both ileum and colon tissues. We assessed intestinal paracellular permeability by in vivo and ex vivo methods, and characterized monocyte-derived and tissue-resident intestinal macrophages by flow cytometry after short, intermediate, and prolonged periods of diet allocation, examining their numbers, prevalence, proliferation, surface marker phenotype, and cytokine profiles. We hypothesized, following from our prior observations of elevated circulating monocytes and adipose tissue macrophages in female mice with diet-induced obesity (17), that there would be an increase in proinflammatory TNF-producing monocyte-derived intestinal macrophages. Furthermore, we predicted that genetic ablation of TNF would not prevent obesity-induced loss of intestinal barrier function or changes to intestinal macrophage populations.

MATERIALS AND METHODS

Ethical Approval

All animal experiments were approved by McMaster University's Animal Research Ethics Board following the recommendations of the Canadian Council on Animal Care.

Animals

All experiments in this study used virgin female mice. Mice were originally purchased from The Jackson Laboratory. Wild-type C57BL/6J mice (Cat. No. 000664; RRID:IMSR_JAX:000664) and tumor necrosis factor knockout (TNF$^{-/-}$) C57BL/6J mice (Cat. No. 003008; RRID:IMSR_JAX:003008) were bred in-house at the McMaster University Central Animal Facility under specific pathogen-free conditions. Littermate TNF$^{+/+}$ and TNF$^{-/-}$ mice were generated from F2 TNF$^{+/-}$ heterozygotes (38), with confirmation of genotype by PCR according to standard protocols of The Jackson Laboratory. Wild-type (WT) mice were weaned onto a standard chow diet (Cat. No. 8640, Teklad 22/5 Rodent Diet, Envigo). Littermate WT and TNF$^{-/-}$ mice were weaned onto Teklad irradiated global 14% protein diet (Cat. No. 2914, Envigo). To assess effects of diet-induced obesity, beginning at 5 wk of age weight-matched WT mice were fed ad libitum a standard chow diet (17% kcal fat, 29% kcal protein, 54% kcal carbohydrates; Teklad 22/5 Rodent Diet) or a high-fat (HF) diet (60% kcal fat, 20% kcal protein, 20% kcal carbohydrates; D12492, Research Diets, Inc.) and provided water ad libitum. To assess effects of TNF in diet-induced obesity, beginning at 8 wk of age littermate TNF$^{+/+}$ and TNF$^{-/-}$ mice were fed ad libitum the HF diet and provided water ad libitum. Mice were cohoused 2–5 per cage with constant ambient temperature (22°C) on a 12-h light-dark cycle under specific pathogen-free conditions. Mice were housed in vent/rack cages with a plastic tube and cotton and paper bedding material for enrichment. Mice were euthanized by exsanguination and/or cervical dislocation under isoflurane anesthesia.

In Vivo Intestinal Paracellular Permeability Assay

Mice were placed in a clean cage and fasted for 6 h before (3 AM to 9 AM) and during the permeability assay. Blood was collected via tail nick using a heparinized capillary tube before gavage (baseline or 0 min sample) with 4 kDa fluorescein isothiocyanate-conjugated dextran (FITC-dextran; Cat. No. 46944, Sigma-Aldrich) diluted in phosphate-buffered saline (PBS, pH 7.4; 80 mg/mL and administered at 500 mg/kg body wt), and again at 30, 60, 90, 120, and/or 240 min post-gavage. Acid-citrate dextrose (15% vol/wt; Cat. No. C3821, Sigma-Aldrich) was added to blood samples after collection to prevent clotting. Plasma was collected post-centrifugation (8,000 rpm, 10 min) after each time point and stored at 4°C until all samples were collected. Fluorescence was measured in plasma diluted 1:10 in PBS, in duplicate, on a plate reader with excitation at 585 nm and emission at 530 nm (Synergy H4 Hybrid Microplate Reader, BioTek Instruments, Inc.). Whole intestine permeability at each time point in each mouse was assessed by subtracting the average relative

fluorescence units of baseline plasma and triplicate wells of PBS (sample blank) from the average postgavage relative fluorescence units.

Ex Vivo Intestinal Paracellular Permeability Assay

Tissues from the proximal colon and distal ileum were excised, opened along the mesenteric border, stripped of the external muscularis layer, and mounted into Ussing chambers (Physiologic Instruments, Inc.), as previously described (39, 40). In brief, samples were equilibrated in oxygenated Krebs buffer containing 10 mM glucose (serosal side) or 10 mM mannitol (luminal side) at 37°C for 30 min. Short-circuit current (I_{sc}) was measured to assess active ion transport. Measurements of potential difference and short-circuit current were used to calculate tissue conductance (G; mS/cm^2) by Ohm's law. Paracellular permeability was determined by measuring mucosal-to-serosal flux (%flux/cm^2/h) of the small inert probe [^{51}Cr]EDTA (ethylenediaminetetraacetic acid; 360 Da; 6 μCi/mL; Perkin Elmer), by taking an initial radiolabeled sample of mucosal buffer and then samples from the serosal compartment every 30 min for 2 h, with addition of fresh buffer to maintain a constant volume. Samples were assessed in a liquid scintillation counter (LS6500 Multi Purpose Scintillation Counter, Beckman Coulter, Inc.), with radioactive counts from each 30-min time point averaged and compared with the initial radiolabeled sample.

Isolation of Primary Cells from Intestinal Tissues for Flow Cytometry

The intestine was collected from stomach to rectum, mesenteric fat was removed, and the intestine was allowed to lay flat. Small intestinal length was measured from the pylorus to the cecum. Colon length was measured from the cecum to the rectum. Ileum and colon tissues were processed for flow cytometry based on previous protocols (4, 41), as described below. The distal 25% of the small intestine adjacent to the cecum was considered ileal tissue. After dissection, intestinal tissue was immediately placed in ice-cold PBS. Peyer's patches (in the small intestine) and mesenteric fat were removed, and the tissue was cut longitudinally and washed with PBS to remove contents. The tissue was cut into ~2-cm pieces and incubated in prewarmed "Stir Media" [RPMI 1640 supplemented with 3% fetal bovine serum (FBS), 100 U/mL penicillin, 100 μg/mL streptomycin, 20 mM HEPES, 5 mM EDTA pH 8.0, and 1 mM dithiothreitol (DTT; Cat. No. D0632, Sigma-Aldrich)] at 37°C for 20 min with constant stirring (~550 rpm) to remove the mucus layer. Tissues were washed 3× by shaking for 30 s in serum-free prewarmed RPMI 1640 supplemented with 100 U/mL penicillin, 100 μg/mL streptomycin, 2 mM EDTA, and 20 mM HEPES and rinsed with prewarmed PBS. The tissue was finely minced with scissors and incubated by stirring in serum-free prewarmed "Complete Media" [RPMI 1640 supplemented with 100 U/mL penicillin, 100 μg/mL streptomycin, 20 mM HEPES, 1% (vol/vol) nonessential amino acids, 1% (vol/vol) sodium pyruvate, 1% (vol/vol) L-glutamine, 0.01% (vol/vol) β-mercaptoethanol], with 0.5 mg/mL DNAse I (Cat. No. 10104159001, Sigma-Aldrich) and 0.1 mg/mL Liberase TL (Cat. No. 05401020001, Sigma-Aldrich) added immediately before incubation for 30 min at 37°C (stirring at ~550 rpm), to dissociate intestinal epithelial cells and leukocytes. Digested tissue was homogenized, washed with ice-cold Stir Media, passed through a 70-μm filter, centrifuged at 1,500 rpm for 10 min, resuspended in ice-cold Stir Media, passed through a 40-μm filter, and centrifuged again at 1,500 rpm for 10 min. The pellet was resuspended in ice-cold Complete Media supplemented with 3% FBS until staining.

Flow Cytometry Analysis

Live cells were counted manually under a light microscope with a hemocytometer and trypan blue (Cat. No. MT25900CI, Corning). Single cell suspensions of 5×10^5 to 2×10^6 cells were stained in a 96 v-well plate, with all centrifugation steps at 2,000 rpm for 2 min. Samples were washed in PBS and were incubated at 4°C with CD16/32 Fc block (Cat. No. 101302, BioLegend) in PBS for 10 min before staining with antibodies (Supplemental Table S1) in PBS for 20 min at 4°C. Samples were washed twice in PBS, fixed for 10 min in 1× eBioscience Fix-Lyse buffer (Cat. No. 00–5333-52, ThermoFisher Scientific), washed in PBS, and resuspended in PBS for flow cytometer analysis. For intracellular staining, samples were stained and fixed as described above, using a modified surface stain (Supplemental Table S2), and then permeabilized in 1× eBioscience Permeabilization Buffer (Cat. No. 88–8824-00, ThermoFisher Scientific) for 30 min at room temperature, stained with intracellular antibody mix (Supplemental Table S3) in 1× Permeabilization Buffer for 30 min, washed twice in PBS, and resuspended in PBS for flow cytometer analysis.

Samples were run on a Fortessa flow cytometer (BD Biosciences). Data were analyzed using the FlowJo v9 software (Tree Star; RRID:SCR_008520). Stained cells were assessed with unstained, isotype, and/or fluorescence-minus-one controls. Expression of surface markers was quantified by measuring geometric mean fluorescence intensity of each fluorescence marker and subtracting background geometric mean fluorescence intensity of unstained controls. Geometric mean expression of each surface marker was combined across multiple independent experiments where noted by normalizing the data. Data was normalized by dividing each geometric mean fluorescence data point by the mean of the comparator group (i.e., chow-fed mice in diet experiments and baseline mice in littermate experiments) for each macrophage population and surface marker in each independent experiment. Absolute cell counts (i.e., total cell numbers) were determined with CountBright Absolute Counting Beads (Cat. No. C36950, Life Technologies) following manufacturer guidelines. Cell numbers were adjusted to tissue length where indicated by dividing the total number of cells by the measured length of the tissue. Flow cytometry data were analyzed as illustrated in Supplemental Fig. S1 for surface staining of intestinal macrophages, and as shown in Supplemental Fig. S2 for intracellular staining of intestinal macrophages.

Statistical Analysis

Data were analyzed and plotted with GraphPad Prism version 9 (GraphPad Software; RRID:SCR_002798). Two-group comparisons of leukocyte populations between diet groups

or genotypes were analyzed by unpaired two-tailed Student's *t* test (parametric) with Welch's correction (for unequal variances) or Mann-Whitney *U* test (nonparametric) according to normality. Comparisons of body weight and intestinal lengths across multiple time points were performed by two-way ANOVA with correction for multiple comparisons by Tukey's test.

RESULTS

Diet-Induced Obesity Decreases Intestinal Length and Increases Paracellular Permeability in Female Mice

Female mice were fed a standard chow diet or HF diet and assessed after short (6 wk), intermediate (12 wk), and prolonged (18 wk) diet consumption, based on turnover rates of intestinal macrophages (4–6). HF-fed mice gained more weight at each time point compared with chow-fed mice (Fig. 1*A*). Decreased intestinal length has often been considered to be an indication of inflammation, and is frequently observed in mouse models of colitis (42) and diet-induced obesity (20, 36, 43, 44). We observed that after short-term diet intake (at 6 wk) small intestine length was decreased in mice fed HF diet (means ± SD: 31.6 ± 1.6 cm) compared with chow-fed mice (35.5 ± 2.8 cm), and this effect persisted with intermediate and prolonged diet allocation (i.e., at 12 and 18 wk; Fig. 1*B*). Colon length was also significantly decreased in HF-fed mice after 6 wk (means ± SD: 6.2 ± 0.4 cm) compared with mice fed chow diet (7.6 ± 1.2 cm) and remained shorter in mice fed HF diet after intermediate and prolonged diet allocation (Fig. 1*C*).

To assess if diet-induced obesity affected intestinal permeability in female mice, we initially performed an in vivo assay by measuring plasma FITC fluorescence after oral gavage of FITC-dextran. Whole intestine paracellular permeability increased in HF-fed mice compared with chow-fed mice with short-term (6 wk) diet allocation, and this increase persisted after prolonged (18 wk) HF diet intake (Fig. 1*D*). We subsequently used an ex vivo short-term organ culture method to examine local tissue permeability in the distal

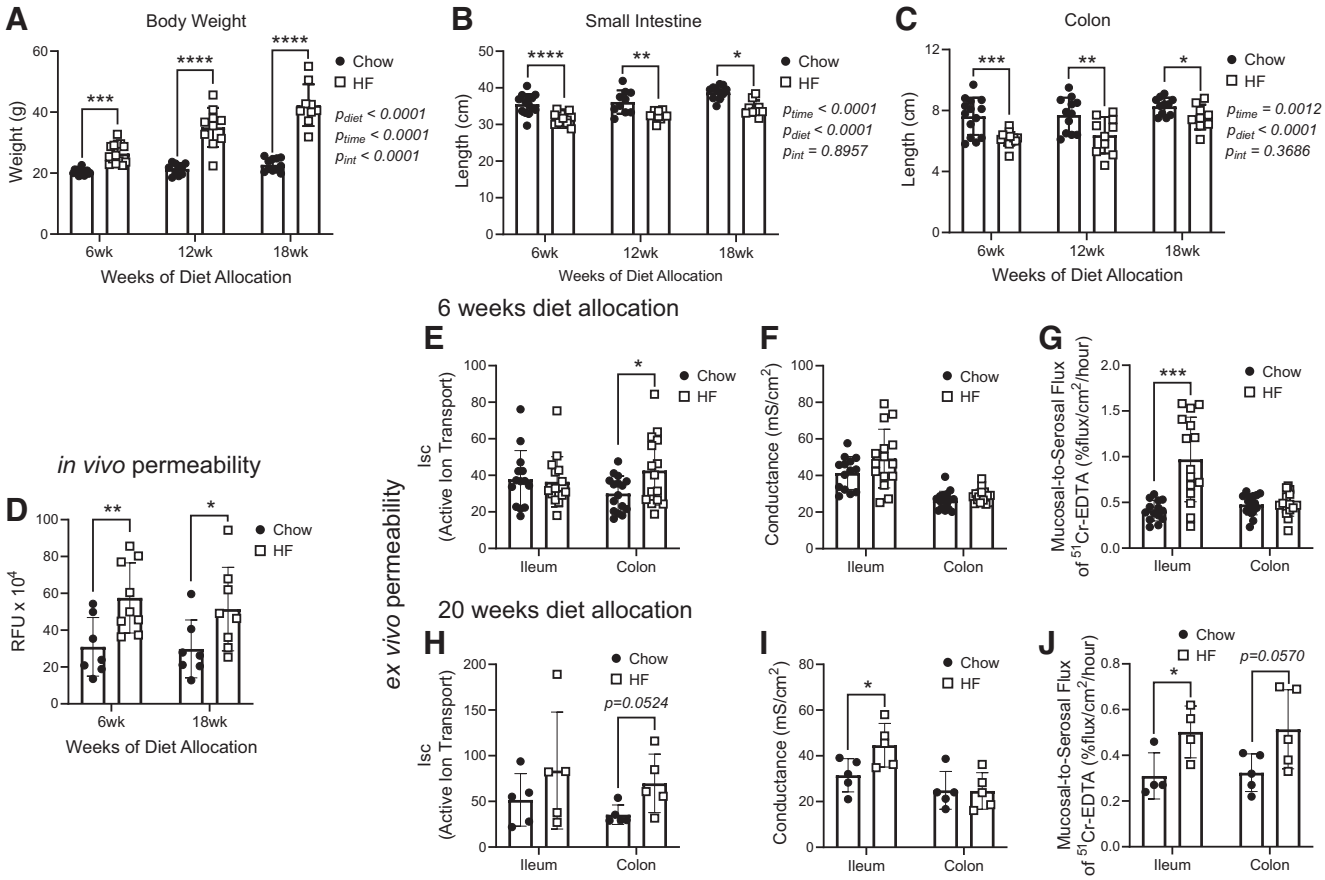

Figure 1. Diet-induced obesity decreases intestinal lengths and increases paracellular permeability in female mice. Body weight, intestinal lengths, and permeability were assessed in mice fed a standard chow (Chow) or high-fat (HF) diet. Body weight (*A*) and lengths of the small intestine (*B*) and colon (*C*) after 6-, 12-, and 18-wk diet allocation. *D*: after 6 and 18 wk of diet allocation, in vivo intestinal permeability to FITC-dextran was measured 4 h after gavage. Ex vivo ileum and colon tissue short-circuit current (I_{sc}) as an indication of active ion transport (*E* and *H*), conductance (*F* and *I*), and paracellular permeability (*G* and *J*), after 6- and 20-wk diet allocation. Each data point indicates an individual mouse. Data are presented with box height at the mean with error bars indicating ± standard deviation. Data in *A*–*C* are combined from 2 or 3 independent experiments of n = 4–5 mice/group (n = 9–14/time point). Data in *D* are representative of 2 independent experiments of n = 7–9 mice/diet group and are presented as relative fluorescence units (RFU). Data in *E*–*G* (6 wk) are combined from 2 independent experiments of n = 8 mice/group. Data in *H*–*J* (20 wk) are from 1 independent experiment of n = 4–5 mice/group. Statistical significance between diet groups was assessed by two-way ANOVA with Tukey's post hoc test for *A*–*C* and by two-tailed Student's *t* test or Welch's *t* test for unequal variances for *D*–*J*. $^*P < 0.05$, $^{**}P < 0.01$, $^{***}P < 0.001$, $^{****}P < 0.0001$. FITC, fluorescein isothiocyanate.

ileum and proximal colon after short (6 wk; Fig. 1, *E–G*) and prolonged (20 wk; Fig. 1, *H–J*) HF diet intake. We measured short-circuit current (I_{sc}; i.e., total ion transport as an indication of fluid and electrolyte homeostasis), conductance (i.e., ion flux in relation to tight junction function), and mucosal-to-serosal flux of [^{51}Cr]EDTA (i.e., paracellular permeability as an indication of tight junction function) (45, 46). Short-circuit current was similar between diet groups after short and prolonged diet allocation in the ileum (Fig. 1, *E* and *H*). Conductance was similar in chow-fed and HF-fed mouse ileum tissues after short-term diet intake (Fig. 1*F*) but increased in HF-fed mouse ileum tissues with longer diet allocation (Fig. 1*I*). Paracellular uptake of [^{51}Cr]EDTA significantly increased in ileum tissues of HF-fed mice compared with chow-fed mice at 6 wk diet intake (Fig. 1*G*) and remained elevated at 20 wk (Fig. 1*J*). In colon tissues of HF-fed mice compared with chow-fed mice, short-circuit current increased after 6 wk diet intake (Fig. 1*E*), and a tendency for higher short-circuit current was also observed after 20 wk (Fig. 1*H*), suggestive of a sustained increase in active ion transport and water movement. Colon tissue conductance was similar between diet groups (Fig. 1, *F* and *I*). Paracellular permeability of colon tissues was similar between diet groups after short-term diet allocation (Fig. 1*G*) but tended to be higher after prolonged HF diet intake (Fig. 1*J*). Therefore, both colon and ileum intestinal barrier changes may contribute to the increased total intestinal permeability observed by in vivo assay after short and prolonged HF diet. These data collectively indicate that intestinal lengths, active ion transport, and paracellular permeability are altered within 6 wk of HF diet consumption. These changes persist or become exacerbated with increasing length of HF diet intake (i.e., after 18–20 wk).

Diet-Induced Obesity Alters Monocyte and Macrophage Dynamics in the Ileum and Colon of Female Mice

We used flow cytometry to assess monocyte and macrophage populations. We initially quantified Ly6C^{high} monocytes, transitional Ly6C$^+$MHCII$^+$ cells, and MHCII$^+$ macrophages in the ileum (Fig. 2, *A–C*) and colon (Fig. 2, *H–J*). The numbers of these cells within the ileum were consistently lower after 6, 12, and 18 wk HF diet intake compared with chow-fed mice (Fig. 2, *A–C*). Similarly, Ly6C^{high} monocyte and total MHCII$^+$ macrophage numbers were lower in colon tissue of HF-fed mice at 6 wk (Fig. 2, *H* and *J*), and Ly6C^{high} monocytes and transitional Ly6C$^+$MHCII$^+$ cells were lower at 12 wk (Fig. 2, *H–I*), compared with chow-fed mice. In contrast, at a prolonged 18 wk of diet allocation, all immune cell populations were similar between diet groups in the colon. Since the lengths of the small intestine and colon were decreased in HF-fed mice (Fig. 1, *B* and *C*), we adjusted cell numbers by tissue length and found similar changes (Supplemental Fig. S3, *A–C* and *G–I*). These data were also evaluated in terms of relative prevalence (as a proportion of total CD45$^+$ leukocytes; Supplemental Fig. S3, *D–F* and *J–L*). In the ileum, the relative prevalence of Ly6C^{high} monocytes was significantly lower at all time points in HF-fed dams, whereas the prevalence of MHCII$^+$ macrophages was consistently increased, but macrophage prevalence did not increase in the colon. Therefore, although we hypothesized there would be an increase in intestinal monocytes and macrophages with diet-induced obesity, the total numbers of Ly6C^{high} monocytes, transitional Ly6C$^+$MHCII$^+$ cells, and total MHCII$^+$ macrophages did not increase in the ileum or colon in female mice with diet-induced obesity after short, intermediate, or prolonged HF diet intake.

The surface markers CD4 and Tim-4 were used to further differentiate ontogenetically and transcriptionally diverse intestinal macrophage populations (4, 5). We examined the quantity (as total cell numbers and cell numbers per tissue length) and prevalence (as a proportion of total macrophages) of monocyte-derived CD4$^-$TIM4$^-$ and CD4$^+$TIM4$^-$ macrophages, as well as tissue-resident CD4$^+$TIM4$^+$ macrophages, in HF-fed and chow-fed mice after 6-, 12-, and 18 wk diet intake (Fig. 2, *D–G* and *K–N*; Supplemental Fig. S4). Consistent with the observed decreases in ileum Ly6C^{high} monocyte and transitional and Ly6C$^+$MHCII$^+$ cell populations, monocyte-derived CD4$^-$TIM4$^-$ macrophage cell numbers (Fig. 2*D*), and cell numbers adjusted to tissue length (Supplemental Fig. S4*A*), were lower in ileal tissue of HF-fed mice compared with chow-fed mice, whether after short, intermediate, or prolonged HF diet allocation. Total cell quantities (and cell numbers adjusted by tissue length) of ileal CD4$^+$TIM4$^-$ macrophage populations were also lower at short and intermediate (i.e., 6 and 12 wk), but not prolonged (18 wk), periods of HF diet intake (Fig. 2*E*; Supplemental Fig. S4*B*). Quantities of tissue-resident CD4$^+$TIM4$^+$ macrophages (but not cell numbers adjusted by tissue length) were also lower at 12 but not 18 wk of HF diet intake (Fig. 2*F*; Supplemental Fig. S4*C*). These changes resulted in a proportional decrease in ileum CD4$^-$TIM4$^-$ macrophages at all assessed time points, and an increase in the prevalence of CD4$^+$TIM4$^-$ macrophages at 12 and 18 wk (Fig. 2*G* and Supplemental Fig. S4, *D–F*). Intramacrophage population dynamics were also altered in the colon. CD4$^+$TIM4$^-$ macrophage numbers, and numbers adjusted by tissue length, were similar between diet groups at all time points (Fig. 2*L*; Supplemental Fig. S4*H*). However, CD4$^+$TIM4$^+$ cell numbers and numbers adjusted by colon tissue length were lower in HF-fed compared with chow-fed mice at 6 and 12 wk but not 18 wk (Fig. 2*M*; Supplemental Fig. S4*I*). These changes resulted in a significantly reduced prevalence of CD4$^+$TIM4$^+$ macrophages and an increase in CD4$^+$TIM4$^-$ macrophages (as a proportion of total macrophages) after 6, 12, and 18 wk of HF diet intake (Fig. 2*N*; Supplemental Fig. S4, *J–L*). Therefore, these data show that there are temporal and tissue-specific changes to intestinal monocyte and macrophage dynamics in response to diet-induced obesity.

Diet-Induced Obesity Does Not Alter Intestinal Macrophage Proliferation in Female Mice but Increases Intracellular IL-10 and Alters Surface Marker Phenotype

In addition to reduced monocyte recruitment, a loss of proliferative capacity could contribute to the reduced quantities of macrophages that we observed in the ileum and colon after HF diet intake. We assessed macrophage proliferation in the ileum and colon by flow cytometry via intracellular staining of the nuclear antigen Ki67 (Fig. 3, *A*, *B*, and *E*). Consistent with prior observations (47), we observed Ki67 expression suggestive of macrophage proliferation. However, there were no

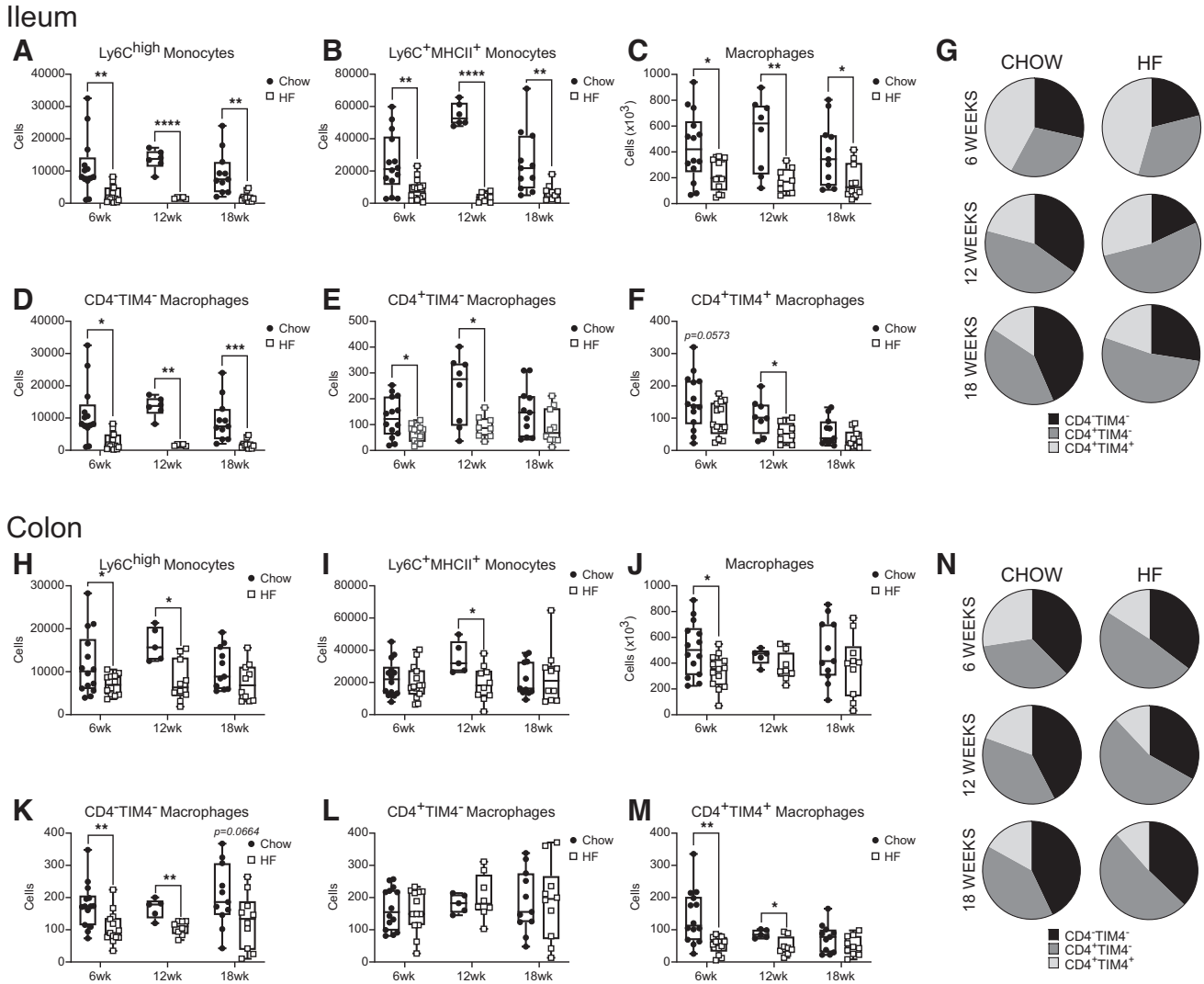

Figure 2. Diet-induced obesity decreases monocytes and macrophages in intestinal tissues in female mice. Intestinal monocyte and macrophage populations were assessed by flow cytometry in the ileum and colon after 6, 12, or 18 wk of standard chow (Chow) or high-fat (HF) diet intake. Ileal absolute cell counts (numbers) of the following: Ly6C^{high} monocytes (*A*), Ly6C^{+}MHCII^{+} cells (*B*), total MHCII^{+} macrophages (*C*), CD4^{-}TIM4^{-} macrophages (*D*), CD4^{+}TIM4^{-} macrophages (*E*), and CD4^{+}TIM4^{+} macrophages (*F*). *G*: summary of average ileum macrophage prevalence (as a proportion of total macrophages; see Supplemental Fig. S4). Colon absolute cell counts (numbers) of the following: Ly6C^{high} monocytes (*H*), Ly6C^{+}MHCII^{+} cells (*I*), total MHCII^{+} macrophages (*J*), CD4^{-}TIM4^{-} macrophages (*K*), CD4^{+}TIM4^{-} macrophages (*L*), and CD4^{+}TIM4^{+} macrophages (*M*). *N*: summary of average colon macrophage prevalence (as a proportion of total macrophages; see Supplemental Fig. S4). Each data point indicates an individual mouse. Data in *A*–*F* and *H*–*M* are presented as box and whisker plots, minimum to maximum, with the centerline at the median. Data are combined from 1 to 3 independent experiments of $n = 4$–5 mice/group. Statistical significance was assessed by two-tailed parametric Student's *t* test or Welch's *t* test for unequal variances or by nonparametric Mann-Whitney *U* test between diet groups at each time point by cell population. $^{*}P < 0.05$, $^{**}P < 0.01$, $^{***}P < 0.001$, $^{****}P < 0.0001$.

statistically significant differences in Ki67 expression between HF and chow diet groups for CD4^{-}TIM4^{-}, CD4^{+}TIM4^{-}, or CD4^{+}TIM4^{+} macrophages in the ileum or colon at any assessed time point. Thus, HF diet-induced obesity did not appear to alter the self-renewal rate of tissue-resident CD4^{+}TIM4^{+} macrophages. Nor was the proliferation of monocyte-derived CD4^{-}TIM4^{-} macrophages, or CD4^{+}TIM4^{-} macrophages, changed in HF-fed mice compared with chow-fed mice, after short, intermediate, or prolonged HF diet intake.

Constitutive expression of IL-10 by intestinal macrophages under homeostatic conditions supports their roles in maintenance of the intestinal barrier and a tolerogenic intestinal environment (48, 49). Intestinal macrophages are also a primary source of TNF. Low levels of TNF are necessary for maintenance of the intestinal epithelium, but higher levels are associated with loss of gut homeostasis (28, 29). We examined intracellular IL-10 and TNF in intestinal macrophages of chow and HF-fed mice in the absence of exogenous stimulation (Fig. 3, *C*–*E*; Supplemental Fig. S5). Consistent with previous studies (11, 50), all intestinal macrophages produced IL-10 as well as TNF, although we found important macrophage population and diet-associated differences. In chow-fed mice, CD4^{+}TIM4^{+} macrophages produced more TNF per cell than CD4^{+}TIM4^{-} or CD4^{-}TIM4^{-} macrophages. There were also temporal changes to IL-10

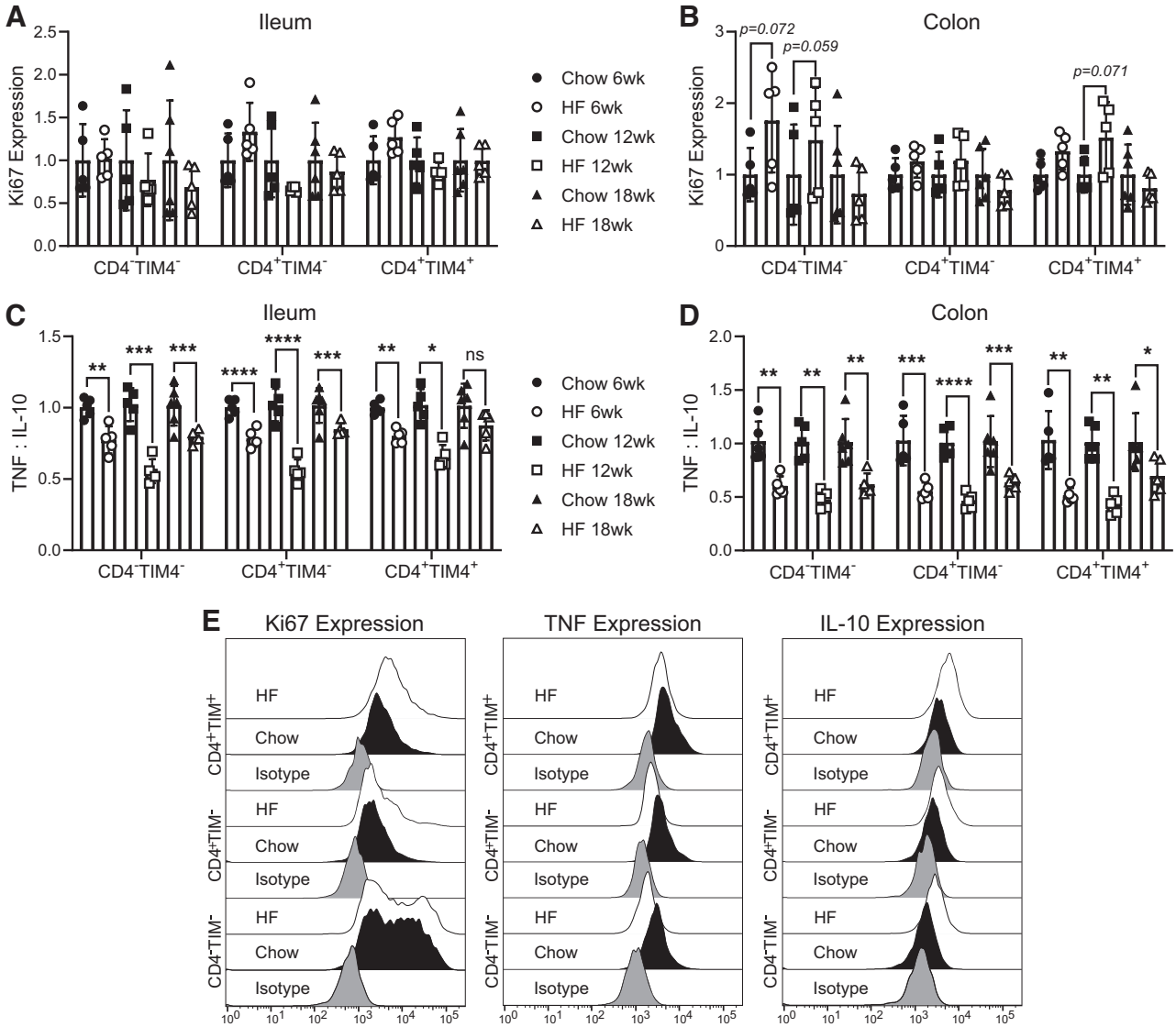

Figure 3. Colon and ileum macrophage proliferation and intracellular production of IL-10 and TNF are altered in obese female mice. Ileum and colon $CD4^{-}TIM4^{-}$, $CD4^{+}TIM4^{-}$, and $CD4^{+}TIM4^{+}$ macrophage proliferation (by Ki67) and intracellular cytokine expression (of TNF and IL-10) was assessed by flow cytometry in standard chow (Chow) or high-fat (HF) diet-fed female mice at 6, 12, or 18 wk of diet intake. Proliferation of macrophages after 6, 12, and 18 wk in the ileum (*A*) and colon (*B*). Ratio of macrophage TNF to IL-10 intracellular expression after 6, 12, and 18 wk in the ileum (*C*) and colon (*D*). *E*: representative expression of Ki67, TNF, and IL-10 in macrophages of chow-fed and HF-fed mice compared with isotype controls. Macrophage proliferation and cytokine expression were compared across lengths of diet allocation (i.e., independent experiments) by normalizing the geometric mean data from each mouse to the mean of the chow mouse group for each macrophage population and surface marker in each independent experiment. Individual cytokine expression measurements of TNF and IL-10 are shown in Supplemental Fig. S5. Each data point indicates an individual mouse. Data are from 1 independent experiment at each time point of $n = 5$–6 mice/group. Data are presented with box height at the mean with error bars at ± standard deviation. Statistical significance was assessed by two-tailed parametric Student's *t* test or Welch's *t* test for unequal variances or by nonparametric Mann–Whitney *U* test between diet groups by macrophage population at each time point. $^{*}P < 0.05$, $^{**}P < 0.01$, $^{***}P < 0.001$, $^{****}P < 0.0001$.

and TNF expression within all macrophage populations from short, intermediate, and prolonged HF diet intake, but intracellular TNF expression in HF-fed mice was not elevated in $CD4^{-}TIM4^{-}$, $CD4^{+}TIM4^{-}$ or $CD4^{+}TIM4^{+}$ macrophages in either the ileum or the colon. Furthermore, the ratio of TNF to IL-10 intracellular expression was lower in intestinal macrophages from HF-fed mice compared with chow-fed mice.

Although our observations of altered intracellular macrophage TNF and IL-10 expression may be suggestive of a more anti-inflammatory role of ileum and colon macrophages after HF diet intake, changes to surface antigen expression can also provide a preliminary assessment of cellular function. We examined ileum and colon macrophage surface expression of Ly6C, CD11b, CD64, CCR2, F4/80, and MHCII (Fig. 4; Supplemental Fig. S6). These surface markers are associated with macrophage migration (CCR2, CD11b), activation (CD11b, F4/80, CD64), phagocytosis and antigen presentation (MHCII), as well as maturity (Ly6C, CD64, F4/80, MHCII) (1, 47, 51–55). Upon arrival into the intestine, newly recruited monocytes differentiate into intestinal tissue macrophages and progressively lose expression of Ly6C and

CCR2 while increasing their expression of CD64, F4/80, and MHCII (56). This assessment revealed significant diet-associated differences in macrophage surface marker phenotype, particularly within the ileum. Ileal $CD4^{-}TIM4^{-}$, $CD4^{+}TIM4^{-}$, and $CD4^{+}TIM4^{+}$ macrophages had reduced surface expression of Ly6C, CD11b, CD64, and CCR2 after short-term (6 wk) and prolonged (18 wk) HF diet intake. Compared with chow-fed mice, MHCII expression was higher on all ileum

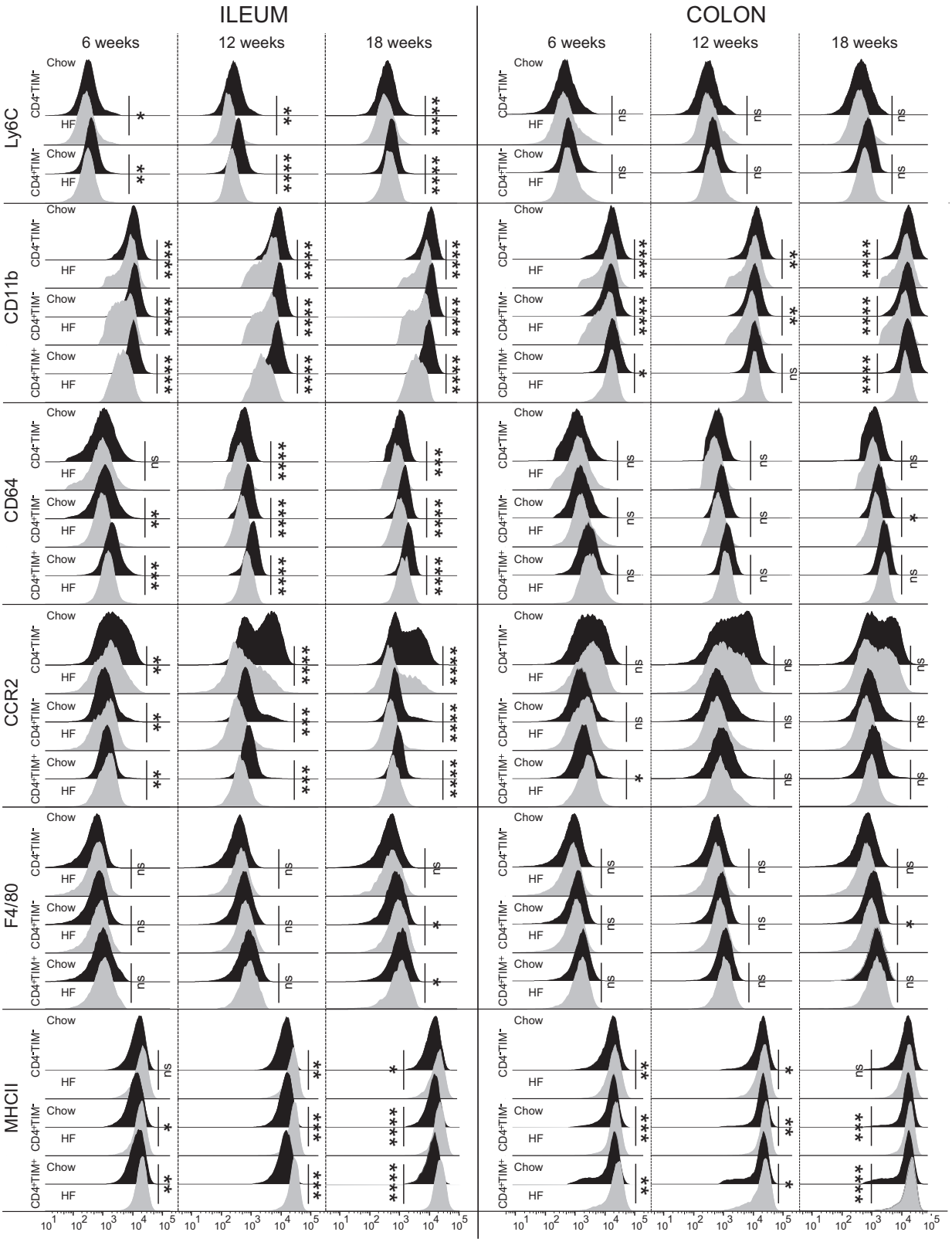

AJP-Gastrointest Liver Physiol • doi:10.1152/ajpgi.00231.2022 • www.ajpgi.org

macrophage populations of HF-fed mice within 12 wk and remained higher at 18 wk. As in the ileum, all colon macrophage populations of HF-fed mice compared with chow-fed mice had lower expression of CD11b within 6 wk of diet intake, which was also apparent after prolonged diet intake at 18 wk, whereas $CD4^+TIM4^-$ and $CD4^+TIM4^+$ macrophages in HF-fed mice had constitutively higher MHCII expression. Colon $CD4^+TIM4^-$ macrophages also had decreased CD64 expression at 18 wk. Therefore, short, intermediate, and prolonged HF diet intake altered the surface marker phenotypes of ileum and colon monocyte-derived $CD4^-TIM^-$ and $CD4^+TIM4^-$ macrophages, as well as tissue-resident $CD4^+TIM4^+$ macrophages. Overall, these data demonstrate that diet-induced obesity results in macrophage subset, tissue, and time-dependent effects on intestinal macrophage surface marker phenotype and intracellular cytokine production.

$TNF^{-/-}$ Female Mice Are Not Protected from Obesity-Induced Changes in Intestinal Length, Paracellular Permeability, or Macrophage Population Dynamics

To assess the involvement of TNF-mediated inflammation in altering intestinal physiology and macrophages in diet-induced obesity, littermate $TNF^{-/-}$ and WT female mice were examined. As we found that intestinal macrophage expression of TNF was lower in HF-fed WT female mice (Fig. 3, *C–E*; Supplemental Fig. S5), and reduced TNF expression in intestinal tissues even in the absence of obesity can be detrimental to epithelial barrier function (28, 29), we hypothesized that genetic ablation of TNF would not protect female mice from intestinal effects of diet-induced obesity. We performed assessments before HF diet allocation (i.e., baseline), or after prolonged periods (15 and 30 wk) of HF diet intake. We observed a main effect of time of HF diet allocation on body weight, but this was independent of genotype (Fig. 5*A*). There were main effects of genotype and time on small intestine lengths (Fig. 5*B*). The small intestines of HF-fed WT mice (means ± SD, 30 wk: 32.1 ± 1.5 cm) were shorter compared with baseline chow-fed WT mice (baseline: 36.3 ± 0.3 cm), as were the small intestine lengths of HF-fed $TNF^{-/-}$ mice (30 wk: 33.1 ± 1.4 cm) compared with baseline chow-fed $TNF^{-/-}$ mice (baseline: 37.9 ± 2.2 cm), though post hoc tests were not significant between genotypes. Although there was no significant effect of genotype on colon length, it decreased with increasing time of HF diet allocation (Fig. 5*C*). In vivo assessments of paracellular permeability showed no significant differences by genotype after 12 wk (Fig. 5*D*) or 28 wk (Fig. 5*E*) of HF diet intake, suggesting that $TNF^{-/-}$ mice had similar whole intestine permeability as WT mice. Together, these data show that in female mice, TNF is not a primary driver of phenotypic changes to body weight, intestinal length, or paracellular permeability, in diet-induced obesity.

We next assessed quantities and relative prevalence of $Ly6C^{high}$ monocytes, transitional $Ly6C^+MHCII^+$ cells, total $MHCII^+$ macrophages, and monocyte-derived ($CD4^-TIM4^-$, $CD4^+TIM4^-$) and tissue-resident ($CD4^+TIM4^+$) macrophage populations in HF-fed WT and $TNF^{-/-}$ mice by flow cytometry (Fig. 6 and Supplemental Fig. S7). There were no significant differences by genotype in the numbers of $Ly6C^{high}$ monocytes (Fig. 6, *A* and *H*), transitional $Ly6C^+MHCII^+$ cells (Fig. 6, *B* and *I*), or $MHCII^+$ macrophages (Fig. 6, *C* and *J*) in either the ileum or colon. The prevalence (as a proportion of total leukocytes) of ileum $Ly6C^{high}$ monocytes and $MHCII^+$ macrophages was also similar in WT and $TNF^{-/-}$ mice, though there was a transient increase in the proportion of colon $Ly6C^{high}$ monocytes after 15 wk in $TNF^{-/-}$ mice (Supplemental Fig. S7, *A–D*). Quantities of monocyte-derived $CD4^-TIM4^-$ and $CD4^+TIM4^-$ macrophages, and tissue-resident $CD4^+TIM4^+$ macrophages, were not significantly different between WT and $TNF^{-/-}$ mice at baseline, or after 15- and 30 wk HF diet intake in either the ileum (Fig. 6, *D–F*) or the colon (Fig. 6, *K–M*). We also considered intramacrophage population prevalence in the ileum (Fig. 6*G*; Supplemental Fig. S7*E*) and colon (Fig. 6*N*; Supplemental Fig. S7*G*). Since there were significant differences between WT and $TNF^{-/-}$ mouse $CD4^+TIM4^-$ and $CD4^+TIM4^+$ macrophage dynamics before diet allocation in both tissues, we also normalized these prevalence data to the mean of the respective genotype group at baseline (Supplemental Fig. S7, *F* and *H*). Although there were some changes in normalized ileum macrophages between genotypes after 30 wk of diet intake, as described above, there were no significant differences in the quantities of cells. These data suggest that similar directional changes in WT and $TNF^{-/-}$ intestinal monocyte-derived and tissue-resident macrophage populations occur in response to HF diet-induced obesity.

We also examined the surface marker phenotypes of intestinal macrophages in HF-fed WT and $TNF^{-/-}$ mice after 15 and 30 wk of diet intake (Fig. 7; Supplemental Fig. S8). Expression of Ly6C, CD11b, CD64, CCR2, F4/80, and MHCII on ileum macrophages was similar between $TNF^{-/-}$ and WT mice after 15 or 30 wk of HF diet feeding. Colon $CD4^+TIM4^+$ macrophages in HF-fed $TNF^{-/-}$ mice compared with WT mice had decreased expression of CD11b after 15 wk, and decreased expression of CD64 after 30 wk, but there were no other significant differences between genotypes. Together our data suggest that in female mice, the absence of TNF does not prevent changes to body weight, intestinal length, paracellular permeability, nor intestinal macrophage numbers or surface marker phenotype that accompany HF diet-induced obesity.

DISCUSSION

In this study we found that diet-induced obesity in female mice has early and sustained effects on intestinal monocytes

Figure 4. Intestinal macrophage surface marker phenotype is altered between chow and high-fat (HF)-fed mice. Flow cytometry analysis of $CD4^-TIM4^-$, $CD4^+TIM4^-$, and $CD4^+TIM4^+$ macrophage populations in the ileums and colons of chow and high-fat (HF)-fed female mice after 6-, 12-, or 18-wk diet allocation. Macrophage phenotype was assessed by examining surface expression of Ly6C, CD11b, CD64, CCR2, F4/80, and MHCII. Data are visualized by concatenating uncompensated events in FlowJo for each mouse and indicated macrophage population at each time point grouped by diet type, and then geometric mean fluorescence intensity expression data of each concatenated group was overlaid onto the same histogram plot. Data of individual mice are plotted in Supplemental Fig. S6. Data are from 2 or 3 independent experiments of $n = 4–5$ mice/group at each time point. Statistical significance was assessed by two-tailed parametric Student's *t* test or Welch's *t* test for unequal variances or by nonparametric Mann-Whitney *U* test between diet groups by macrophage population at each time point. $^*P < 0.05$, $^{**}P < 0.01$, $^{***}P < 0.001$, $^{****}P < 0.0001$.

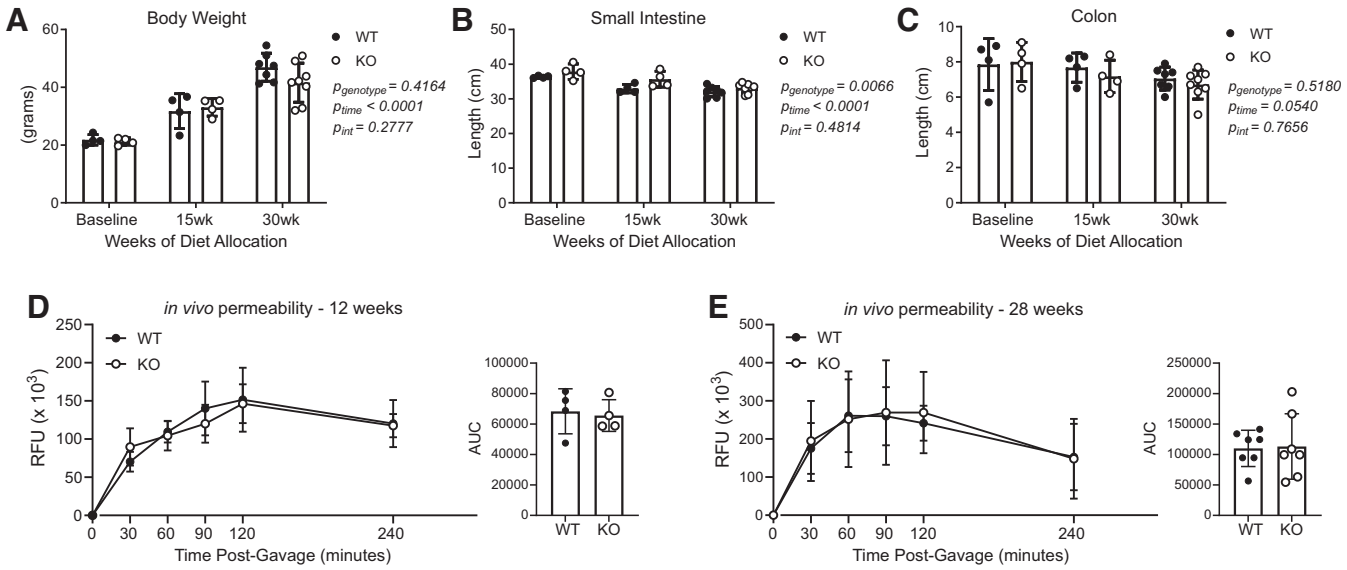

Figure 5. TNF does not impact body weight, intestine lengths or paracellular permeability in HF-fed female mice. Littermate wild-type (WT) and $TNF^{-/-}$ (KO) mice were assessed before diet allocation (baseline) and after allocation to a high-fat diet for up to 15 wk (15wk) or 30 wk (30wk). *A*: body weight. *B*: small intestine length. *C*: colon length. In vivo intestinal permeability to FITC-dextran after 12 wk diet allocation (*D*) and 28 wk diet allocation (*E*). Data in *A*–*C* are presented with box height at the mean and error bars at ± standard deviation, and each data point indicates an individual mouse. Data in *D* and *E* are presented as relative fluorescence units (RFU) with a dot at the means ± standard deviation, with area under the curve (AUC) presented with box height at the mean with error bars indicating ± standard deviation and each data point indicating an individual mouse. Data are from independent experiments of WT n = 4 and KO n = 4 at 15 wk, and WT n = 7 and KO n = 8 at 30 wk. Statistical significance was assessed between genotypes at each time point by two-way ANOVA with Tukey's post hoc test for A–C and by two-tailed Student's t test and AUC for *D* and *E*. FITC, fluorescein isothiocyanate; HF, high fat; KO, knockout.

and macrophages, including a decrease in monocyte recruitment, and depletion of monocyte-derived macrophages as well as tissue-resident macrophages, without a subsequent compensatory increase in local macrophage proliferation. Our data confirm that the recruitment, phenotype, and functions of intestinal monocytes and macrophages are affected by changes within their local tissue microenvironment (57) and support previous observations of altered intestinal macrophage populations in obese humans (58, 59). We observed that monocyte-derived and tissue-resident intestinal macrophages in female mice with diet-induced obesity do not have increased intracellular expression of TNF. Increased adipose tissue macrophage accumulation and elevated macrophage production of TNF have been associated with local and systemic inflammation as well as metabolic dysregulation in diet-induced obesity (18, 19, 60). Our data contrast with these observations and reports of accumulation of proinflammatory TNF-producing monocyte-derived macrophages within the intestines in response to acute or chronic inflammation from infection or colitis (10–12). Nonetheless, our data are consistent with histological reports of low-grade inflammation in the intestines compared with metabolic tissues in obesity (21, 61), as well as with observations of the ability of intestinal macrophages to remain hyporesponsive to exogenous stimulation (57, 62). Therefore, our findings are reflective of the intrinsically anti-inflammatory and tolerogenic environment of the gut (63). Although outside the scope of this study, further research that incorporates in situ immunohistochemistry or immunofluorescence techniques would provide further insight into any spatially restricted changes in intestinal macrophage populations. It is also possible that there are proinflammatory shifts in other intestinal immune cells in response to diet-induced obesity, as has been reported for some T cell populations (24, 58, 61), which may influence macrophage composition and function.

We found that HF diet-induced obesity results in tissue- and time-dependent physiological changes within the intestines, including shortening of ileum and colon lengths, increased colon ion transport, and elevated paracellular permeability. These data support prior literature showing that diet-induced obesity impairs maintenance of the intestinal epithelium (20–23, 64). Diet-induced obesity has also been reported to dysregulate blood vessel barriers (65), enteric neuron activity (66), and gastrointestinal motility (67). As all of these functions are affected by disruption of monocyte recruitment and/or macrophage depletion (5, 9, 68, 69), an obesity-associated reduction in intestinal monocyte and macrophage numbers, as observed in this study, may contribute to those physiological changes. Furthermore, as mentioned, under homeostatic conditions TNF regulates intestinal epithelial barrier function (28). Although overproduction of TNF is typically associated with damage to the intestinal epithelium, it has been demonstrated that tissue-resident macrophage production of TNF is actually protective against colitis induced by disruption of the intestinal epithelium (70). Our data suggest that intestinal macrophages do not contribute to local inflammation via TNF in diet-induced obesity, yet the decrease in relative TNF production by both ileum and colon macrophages that we found in HF-fed mice may have contributed to the observed increases in paracellular permeability. Thus, obesity-associated loss of intestinal homeostasis is likely mediated by physiological changes that contribute to alterations in local macrophage populations, and vice versa.

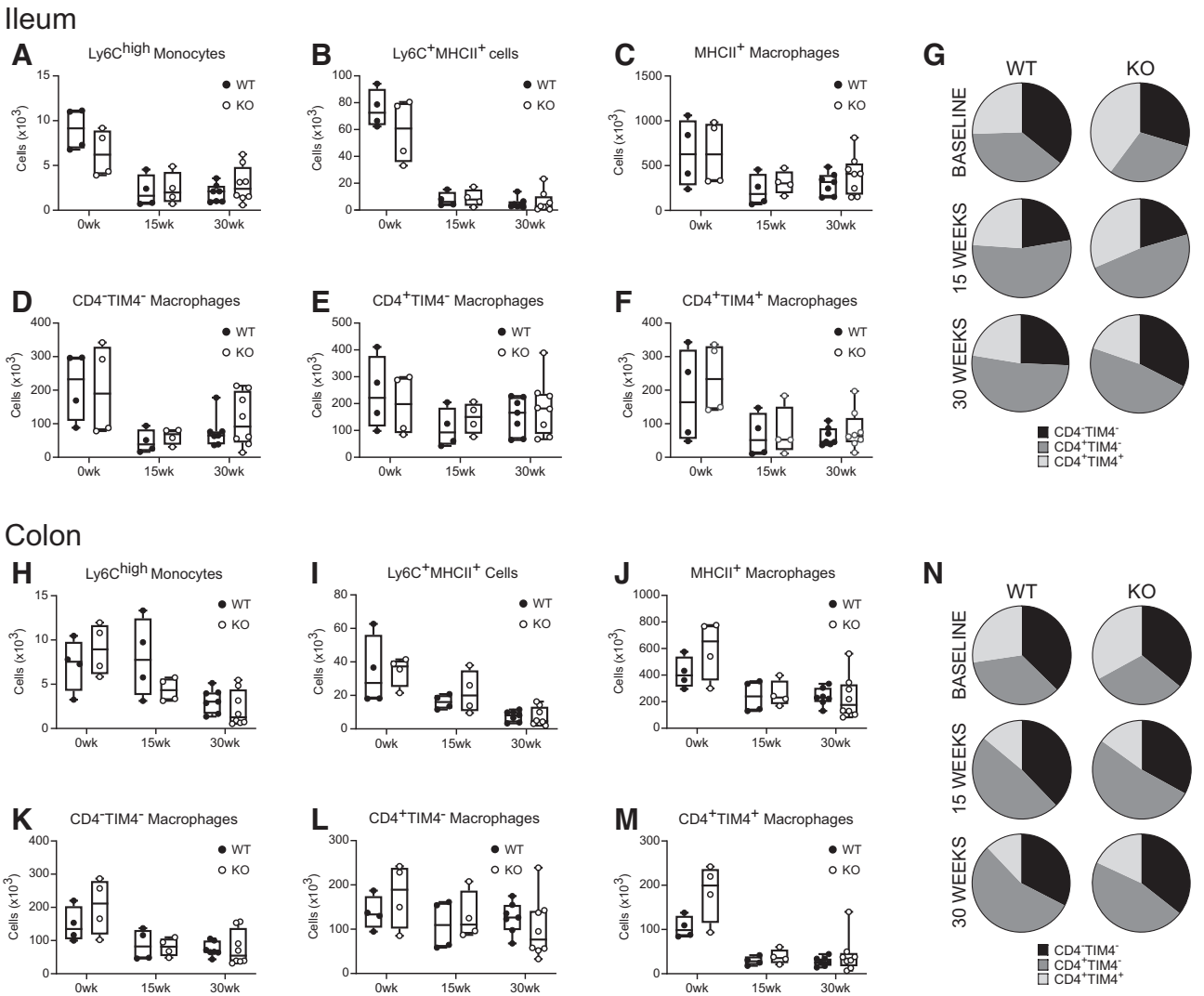

Figure 6. TNF does not impact effects of diet-induced obesity on intestinal monocytes and macrophages in female mice. Littermate wild-type (WT) and TNF$^{-/-}$ (KO) mice were assessed before diet allocation (baseline) and after allocation to a high-fat diet for up to 15 wk (15wk) or 30 wk (30wk). Intestinal monocyte and macrophage populations were assessed by flow cytometry in the colon and ileum. Ileum absolute cell counts (numbers) of Ly6C^{high} monocytes (*A*), Ly6C$^+$MHCII$^+$ cells (*B*), total MHCII$^+$ macrophages (*C*), CD4$^-$TIM4$^-$ macrophages (*D*), CD4$^+$TIM4$^-$ macrophages (*E*), and CD4$^+$TIM4$^+$ macrophages (*F*). *G*: summary of ileum average macrophage prevalence (as a proportion of total macrophages; also see Supplemental Fig. S7). Colon absolute cell counts (numbers) of Ly6C^{high} monocytes (*H*), Ly6C$^+$MHCII$^+$ cells (*I*), total MHCII$^+$ macrophages (*J*), CD4$^-$TIM4$^-$ macrophages (*K*), CD4$^+$TIM4$^-$ macrophages (*L*), and CD4$^+$TIM4$^+$ macrophages (*M*). *N*: summary of colon average macrophage prevalence (as a proportion of total macrophages; also see Supplemental Fig. S7). Each data point indicates an individual mouse. Data in *A*–*F* and *H*–*M* are presented as box and whisker plots, minimum to maximum, with the centerline at the median. Data are from independent experiments of WT $n = 4$ and KO $n = 4$ at 15 wk, and WT $n = 7$ and KO $n = 8$ at 30 wk. Statistical significance was assessed by two-tailed parametric Student's *t* test or Welch's *t* test for unequal variances or by nonparametric Mann–Whitney *U* test between genotypes by cell population at each time point. KO, knockout.

Obesity-associated changes to the microbiota and microbial metabolite production may also influence local macrophage populations (71). In addition, it should be noted that saturated fatty acids found in HF diets can induce macrophage mitochondrial dysfunction and apoptosis (72, 73). Exacerbated pathology has been reported after high-fat diet feeding in mouse models of colitis in the absence of obesity (74, 75). Most dietary fats are absorbed in the small intestine (63), which may explain why we observed a greater and more sustained depletion of monocyte-derived macrophages and increase in paracellular permeability in the ileum compared with the colon. Given the ubiquitous use of HF diets in mouse models of obesity, consideration of independent and combined effects of diet and obesity on intestinal macrophages and other immune cells merits further research. Irrespective, our data align with previous work showing that diet-induced obesity results in loss of intestinal homeostasis and barrier function (20, 23, 26), which may promote translocation of luminal contents including bacterial products into circulation that contribute to the gradual development of systemic inflammation and metabolic dysfunction.

The gut is a dynamic organ, which experiences natural changes in structure, function, and immune cell composition throughout the life course (76). In young chow-fed mice, we observed a gradual increase in the prevalence of monocyte-derived macrophages and an accompanying decrease

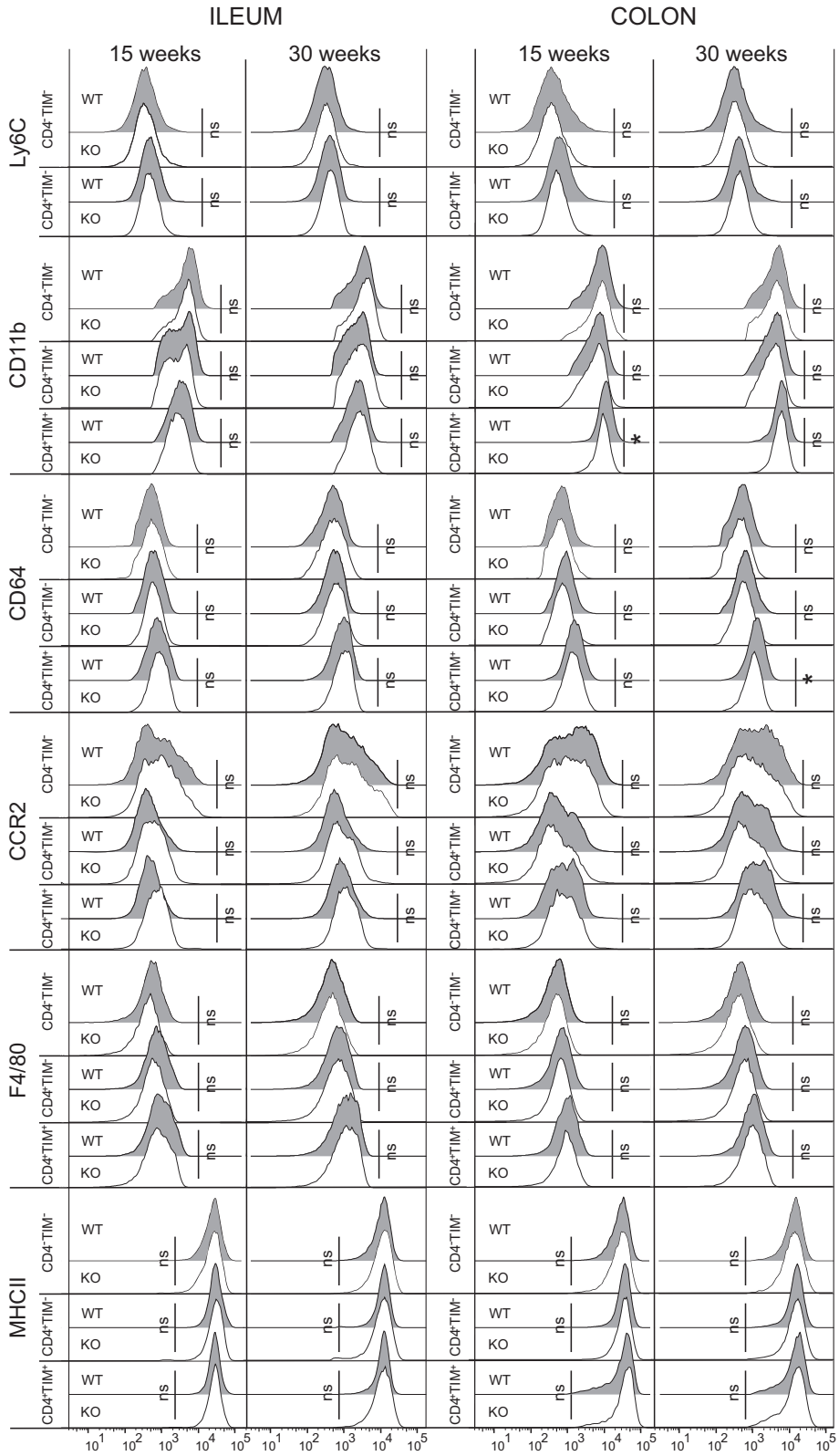

Figure 7. TNF does not mediate changes to macrophage surface marker phenotype in HF-fed female mice. Flow cytometry analysis of $CD4^{-}TIM4^{-}$, $CD4^{+}TIM4^{-}$, and $CD4^{+}TIM4^{+}$ macrophage populations in the ileums and colons of littermate wild-type (WT) and $TNF^{-/-}$ (KO) female mice on high-fat diet for 15 or 30 wk. Macrophage phenotype was assessed by examining surface expression of Ly6C, CD11b, CD64, CCR2, F4/80, and MHCII. Data are reported as geometric mean fluorescence intensity and are visualized by concatenating uncompensated events in FlowJo for each mouse and indicated macrophage population at each time point grouped by genotype, and then geometric mean fluorescence intensity expression data of each concatenated group was overlaid onto the same histogram plot. Data of individual mice are plotted in Supplemental Fig. S8. Data are from independent experiments of WT $n = 4$ and KO $n = 4$ at 15 wk, and WT $n = 7$ and KO $n = 8$ at 30 wk. Statistical significance was assessed by two-tailed parametric Student's t test or Welch's t test for unequal variances or by nonparametric Mann–Whitney U test between genotypes by macrophage population at each time point. $^{*}P < 0.05$. HF, high fat; KO, knockout.

in the prevalence of tissue-resident macrophages within ileum and colon tissues between the short, intermediate, and prolonged time points of assessment between 6 and 18 wk. These data are consistent with previous reports of macrophage population composition and turnover, showing that there is a gradual increase in monocyte-derived macrophages in intestinal (and other) tissues from birth in mice (4, 6) and in humans (77–79). Accordingly, the disruptions in monocyte-derived and tissue-resident macrophage turnover dynamics that we observed due to HF diet-induced obesity

could have more severe long-term effects on intestinal function if they occur earlier in life than in mature adults (i.e., before stabilization of intestinal macrophage populations). Further studies should consider if effects of diet-induced obesity on intestinal macrophages differ in contexts that impact intestinal function and permeability, including pregnancy and lactation (80), increasing age (81), and when homeostasis is already disturbed, such as in response to acute or chronic inflammation (42, 82).

We observed that monocyte-derived and tissue-resident intestinal macrophages in female mice with diet-induced obesity have tissue and time-dependent increases in intracellular expression of the anti-inflammatory cytokine IL-10. Colon macrophages of HF-fed mice in particular had elevated IL-10 expression after short and intermediate (i.e., 6 and 12 wk), but not prolonged (i.e., 18 wk), diet allocation. Given the established importance of IL-10 in maintenance of cellular function, immunological tolerance, and the intestinal barrier (83), these observations may indicate that increased IL-10 production by intestinal macrophages is an early response to HF diet consumption that promotes restoration of intestinal homeostasis. It has been previously reported that IL-10$^{-/-}$ mice fed a HF diet have exacerbated pathology in the colon (84), but it is unclear whether macrophage-specific depletion of IL-10 has a similar effect. HF-fed mice with knockout of hematopoietic cell-derived IL-10 do not have adipose or liver tissue inflammation (85), though to our knowledge intestinal tissues have not been examined to date. Therefore, additional investigation is merited to examine IL-10 production by intestinal macrophages and its possible roles in protection against obesity-associated inflammation and dysregulation of intestinal function.

Our finding that TNF did not contribute to changes in intestinal physiology and macrophages in HF diet-induced obesity was unexpected, because previous research suggests that TNF contributes to intestinal inflammation in diet-induced obesity (20, 35–37). Yet, there are conflicting data from animal models and clinical reports on TNF and anti-TNF therapies, implying that TNF has pleiotropic effects in acute and chronic inflammation within the intestines. For example, TNF$^{-/-}$ mice are not susceptible to acute or chronic TNBS-induced colitis (86) but are susceptible to acute dextran sulfate sodium (DSS)-induced colitis (87). As well, anti-TNF therapy leads to worse tissue damage in acute DSS-colitis (88), but reduces inflammation in chronic colitis (87). Treatment failure of anti-TNF therapy is documented in inflammatory bowel disease, with both primary nonresponse or loss of response after initial successful treatment (89), which suggests that there may be different etiologies of intestinal inflammation that are not TNF dependent. Collectively, these data caution that context may dictate whether TNF has beneficial or deleterious effects. Proinflammatory TNF-producing macrophages are plentiful in obese adipose tissue, and the absence of these macrophages attenuates obesity-associated immunometabolic dysfunction (18–20, 60). Yet, whole body adiposity and systemic metabolic dysregulation were not significantly reduced in male mouse models of diet-induced obesity after ablation of immune cell and myeloid-specific TNF production (i.e., via TNF$^{-/-}$ bone marrow transplantation into WT mice or LysMcre-based deletion of TNF) (90, 91). Although these observations caution that other endogenous sources of TNF and macrophage-associated factors contribute to systemic effects of diet-induced obesity, modulating TNF production from specific cell populations may also provide further insight into the local roles of macrophage TNF production within intestinal tissues in obesity.

Intestinal effects of TNF could in addition be further modified by biological sex, which influences both immunity and metabolism (92, 93). It has been reported that TNF-producing monocyte-derived colon macrophages promote obesity-associated metabolic dysfunction in male mice (20, 27). However, we have observed that although both obese male and female mice have an increase in circulating inflammatory TNF-producing Ly6C^{high} monocytes and adipose tissue macrophage accumulation, in female mice the metabolic dysregulation is attenuated, and these changes are not dependent on TNF (16, 93). Although turnover of intestinal macrophages has been reported to be similar in nonobese young male and female mice (6, 94), it has been found that estrogen treatment has anti-inflammatory effects in mouse models of colitis (95, 96), and moreover, estrogen may attenuate effects of diet-induced obesity in the colon (97). A priori consideration of biological sex and hormones may therefore be indispensable in disentangling the complex effects of TNF in both acute and chronic intestinal inflammation. Future investigations should be designed to evaluate how estrogens and androgens modify the role of TNF in mediating changes to intestinal macrophage populations and maintenance of the intestinal barrier in obesity.

In conclusion, we have identified tissue-specific effects of diet-induced obesity on monocyte-derived and tissue-resident intestinal macrophage numbers, prevalence, proliferation, surface marker phenotype, and cytokine profiles. These data emphasize the importance of studying macrophages within their local tissue environment, and contribute to the growing evidence that biological sex influences cellular immune responses to obesity-associated chronic inflammation.

DATA AVAILABILITY

Data will be made available upon reasonable request.

SUPPLEMENTAL DATA

Supplemental Tables S1–S3 and Supplemental Figs. S1–S8: https://doi.org/10.6084/m9.figshare.22041587.v1.

ACKNOWLEDGMENTS

The authors thank John Grainger for guidance on tissue processing and flow cytometry protocol design; Tatiane Ribeiro for guidance on in vivo permeability assays; as well as Erica Yeo, Erica DeJong, Janine Strehmel, Melodie Kim, Brianna Kennelly, and Braeden Cowbrough for technical support; Hong Liang and the McMaster Immunology Research Centre flow cytometry facility; and Erin Demask and Tina Walker for provision of media. The graphical abstract was created using BioRender.com.

GRANTS

This work was funded by a Team Grant from the Canadian Institutes of Health Research (CIHR) led by D.M.S. J.A.B. was

supported by a Queen Elizabeth II Scholarship in Science and Technology. Work in the Bowdish laboratory was supported by the CIHR, the McMaster Immunology Research Centre, and the M. G. DeGroote Institute for Infectious Disease Research. Work in the Verdú laboratory was supported by the Farncombe Family Digestive Health Research Institute. E.F.V., D.M.E.B., and D.M.S. hold Canada Research Chairs.

DISCLOSURES

No conflicts of interest, financial or otherwise, are declared by the authors.

AUTHOR CONTRIBUTIONS

J.A.B., D.M.S., and D.M.E.B. conceived and designed research; J.A.B. and J.J. performed experiments; J.A.B. and J.J. analyzed data; J.A.B., J.J., E.F.V., D.M.S., and D.M.E.B. interpreted results of experiments; J.A.B. prepared figures; J.A.B. drafted manuscript; J.A.B., E.F.V., D.M.S., and D.M.E.B. edited and revised manuscript; J.A.B., E.F.V., D.M.S., and D.M.E.B. approved final version of manuscript.

REFERENCES

1. **Gordon S**, **Plüddemann A.** The mononuclear phagocytic system. Generation of diversity. *Front Immunol* 10: 1893, 2019. doi:10.3389/fimmu.2019.01893.
2. **Medzhitov R.** Origin and physiological roles of inflammation. *Nature* 454: 428–435, 2008. doi:10.1038/nature07201.
3. **McNelis JC**, **Olefsky JM.** Macrophages, immunity, and metabolic disease. *Immunity* 41: 36–48, 2014. doi:10.1016/j.immuni.2014.05.010.
4. **Shaw TN**, **Houston SA**, **Wemyss K**, **Bridgeman HM**, **Barbera TA**, **Zangerle-Murray T**, **Strangward P**, **Ridley AJL**, **Wang P**, **Tamoutounour S**, **Allen JE**, **Konkel JE**, **Grainger JR.** Tissue-resident macrophages in the intestine are long lived and defined by Tim-4 and CD4 expression. *J Exp Med* 215: 1507–1518, 2018. doi:10.1084/jem.20180019.
5. **De Schepper S**, **Verheijden S**, **Aguilera-Lizarraga J**, **Viola MF**, **Boesmans W**, **Stakenborg N**, **Voytyuk I**, **Schmidt I**, **Boeckx B**, **Dierckx de Casterlé I**, **Baekelandt V**, **Gonzalez Dominguez E**, **Mack M**, **Depoortere I**, **De Strooper B**, **Sprangers B**, **Himmelreich U**, **Soenen S**, **Guilliams M**, **Vanden Berghe P**, **Jones E**, **Lambrechts D**, **Boeckxstaens G.** Self-maintaining gut macrophages are essential for intestinal homeostasis. *Cell* 175: 400–415.e13, 2018. doi:10.1016/j.cell.2018.07.048.
6. **Liu Z**, **Gu Y**, **Chakarov S**, **Bleriot C**, **Kwok I**, **Chen X**, **Shin A**, **Huang W**, **Dress RJ**, **Dutertre C-A**, **Schlitzer A**, **Chen J**, **Ng LG**, **Wang H**, **Liu Z**, **Su B**, **Ginhoux F.** Fate mapping via Ms4a3-expression history traces monocyte-derived cells. *Cell* 178: 1509–1525.e19, 2019. doi:10.1016/j.cell.2019.08.009.
7. **Hume DA**, **Perry VH**, **Gordon S.** The mononuclear phagocyte system of the mouse defined by immunohistochemical localisation of antigen F4/80: macrophages associated with epithelia. *Anat Rec* 210: 503–512, 1984. doi:10.1002/ar.1092100311.
8. **Mikkelsen H**, **Mirsky R**, **Jessen K**, **Thuneberg L.** Macrophage-like cells in muscularis externa of mouse small intestine: immunohistochemical localization of F4/80, M1/70, and Ia-antigen. *Cell Tissue Res* 252: 301–306, 1988. doi:10.1007/BF00214372.
9. **Gabanyi I**, **Muller PA**, **Feighery L**, **Oliveira TY**, **Costa-Pinto FA**, **Mucida D.** Neuro-immune interactions drive tissue programming in intestinal macrophages. *Cell* 164: 378–391, 2016. doi:10.1016/j.cell.2015.12.023.
10. **Zigmond E**, **Varol C**, **Farache J**, **Elmaliah E**, **Satpathy AT**, **Friedlander G**, **Mack M**, **Shpigel N**, **Boneca IG**, **Murphy KM**, **Shakhar G**, **Halpern Z**, **Jung S.** Ly6C hi monocytes in the inflamed colon give rise to proinflammatory effector cells and migratory antigen-presenting cells. *Immunity* 37: 1076–1090, 2012. doi:10.1016/j.immuni.2012.08.026.
11. **Bain CC**, **Scott CL**, **Uronen-Hansson H**, **Gudjonsson S**, **Jansson O**, **Grip O**, **Guilliams M**, **Malissen B**, **Agace WW**, **Mowat AM.** Resident and pro-inflammatory macrophages in the colon represent alternative context-dependent fates of the same Ly6Chi monocyte precursors. *Mucosal Immunol* 6: 498–510, 2013. doi:10.1038/mi.2012.89.
12. **Bain CC**, **Oliphant CJ**, **Thomson CA**, **Kullberg MC**, **Mowat AM.** Proinflammatory role of monocyte-derived CX3CR1(int) macrophages in helicobacter hepaticus-induced colitis. *Infect Immun* 86: e00579-17, 2018. doi:10.1128/IAI.00579-17.
13. **Qualls JE**, **Kaplan AM**, **van Rooijen N**, **Cohen DA.** Suppression of experimental colitis by intestinal mononuclear phagocytes. *J Leukoc Biol* 80: 802–815, 2006. doi:10.1189/jlb.1205734.
14. **Weber B**, **Saurer L**, **Schenk M**, **Dickgreber N**, **Mueller C.** CX3CR1 defines functionally distinct intestinal mononuclear phagocyte subsets which maintain their respective functions during homeostatic and inflammatory conditions. *Eur J Immunol* 41: 773–779, 2011. doi:10.1002/eji.201040965.
15. **Hotamisligil GS.** Inflammation, metaflammation and immunometabolic disorders. *Nature* 542: 177–185, 2017. doi:10.1038/nature21363.
16. **Breznik JA**, **Naidoo A**, **Foley KP**, **Schulz C**, **Lau TC**, **Loukov D**, **Sloboda DM**, **Bowdish DME**, **Schertzer JD.** TNF, but not hyperinsulinemia or hyperglycemia, is a key driver of obesity-induced monocytosis revealing that inflammatory monocytes correlate with insulin in obese male mice. *Physiol Rep* 6: e13937, 2018. doi:10.14814/phy2.13937.
17. **Breznik JA**, **Foley KP**, **Maddiboina D**, **Schertzer JD**, **Sloboda DM**, **Bowdish DME.** Effects of obesity-associated chronic inflammation on peripheral blood immunophenotype are not mediated by TNF in female C57BL/6J mice. *Immunohorizons* 5: 370–383, 2021. doi:10.4049/immunohorizons.2100038.
18. **Weisberg SP**, **McCann D**, **Desai M**, **Rosenbaum M**, **Leibel RL**, **Ferrante AW Jr.** Obesity is associated with macrophage accumulation in adipose tissue. *J Clin Invest* 112: 1796–1808, 2003. doi:10.1172/JCI19246.
19. **Kanda H**, **Tateya S**, **Tamori Y**, **Kotani K**, **Hiasa K**, **Kitazawa R**, **Kitazawa S**, **Miyachi H**, **Maeda S**, **Egashira K**, **Kasuga M.** MCP-1 contributes to macrophage infiltration into adipose tissue, insulin resistance, and hepatic steatosis in obesity. *J Clin Invest* 116: 1494–1505, 2006. doi:10.1172/JCI26498.
20. **Kawano Y**, **Nakae J**, **Watanabe N**, **Kikuchi T**, **Tateya S**, **Tamori Y**, **Kaneko M**, **Abe T**, **Onodera M**, **Itoh H.** Colonic pro-inflammatory macrophages cause insulin resistance in an intestinal Ccl2/Ccr2-dependent manner. *Cell Metab* 24: 295–310, 2016. doi:10.1016/j.cmet.2016.07.009.
21. **Johnson AM**, **Costanzo A**, **Gareau MG**, **Armando AM**, **Quehenberger O**, **Jameson JM**, **Olefsky JM.** High fat diet causes depletion of intestinal eosinophils associated with intestinal permeability. *PLoS One* 10: e0122195, 2015. doi:10.1371/journal.pone.0122195.
22. **Cani PD**, **Amar J**, **Iglesias MA**, **Poggi M**, **Knauf C**, **Bastelica D**, **Neyrinck AM**, **Fava F**, **Tuohy KM**, **Chabo C**, **Waget A**, **Delmée E**, **Cousin B**, **Sulpice T**, **Chamontin B**, **Ferrières J**, **Tanti JF**, **Gibson GR**, **Casteilla L**, **Delzenne NM**, **Alessi MC**, **Burcelin R.** Metabolic endotoxemia initiates obesity and insulin resistance. *Diabetes* 56: 1761–1772, 2007. doi:10.2337/db06-1491.
23. **Cani PD**, **Delzenne NM**, **Amar J**, **Burcelin R.** Role of gut microflora in the development of obesity and insulin resistance following high-fat diet feeding. *Pathol Biol (Paris)* 56: 305–309, 2008. doi:10.1016/j.patbio.2007.09.008.
24. **Garidou L**, **Pomié C**, **Klopp P**, **Waget A**, **Charpentier J**, **Aloulou M**, **Giry A**, **Serino M**, **Stenman L**, **Lahtinen S**, **Dray C**, **Iacovoni JS**, **Courtney M**, **Collet X**, **Amar J**, **Servant F**, **Lelouvier B**, **Valet P**, **Eberl G**, **Fazilleau N**, **Douin-Echinard V**, **Heymes C**, **Burcelin R.** The gut microbiota regulates intestinal CD4 T cells expressing RORγt and controls metabolic disease. *Cell Metab* 22: 100–112, 2015. doi:10.1016/j.cmet.2015.06.001.
25. **Hong CP**, **Park A**, **Yang BG**, **Yun CH**, **Kwak MJ**, **Lee GW**, **Kim JH**, **Jang MS**, **Lee EJ**, **Jeun EJ**, **You G**, **Kim KS**, **Choi Y**, **Park JH**, **Hwang D**, **Im SH**, **Kim JF**, **Kim YK**, **Seoh JY**, **Surh CD**, **Kim YM**, **Jang MH.** Gut-specific delivery of T-helper 17 cells reduces obesity and insulin resistance in mice. *Gastroenterology* 152: 1998–2010, 2017. doi:10.1053/j.gastro.2017.02.016.
26. **Luck H**, **Khan S**, **Kim JH**, **Copeland JK**, **Revelo XS**, **Tsai S**, **Chakraborty M**, **Cheng K**, **Tao Chan Y**, **Nøhr MK**, **Clemente-Casares X**, **Perry MC**, **Ghazarian M**, **Lei H**, **Lin YH**, **Coburn B**, **Okrainec A**, **Jackson T**, **Poutanen S**, **Gaisano H**, **Allard JP**, **Guttman DS**, **Conner ME**, **Winer S**, **Winer DA.** Gut-associated IgA

(+) immune cells regulate obesity-related insulin resistance. *Nat Commun* 10: 3650, 2019. doi:10.1038/s41467-019-11370-y.

27. **Rohm TV**, **Keller L**, **Bosch AJT**, **AlAsfoor S**, **Baumann Z**, **Thomas A**, **Wiedemann SJ**, **Steiger L**, **Dalmas E**, **Wehner J**, **Rachid L**, **Mooser C**, **Yilmaz B**, **Fernandez Trigo N**, **Jauch AJ**, **Wueest S**, **Konrad D**, **Henri S**, **Niess JH**, **Hruz P**, **Ganal-Vonarburg SC**, **Roux J**, **Meier DT**, **Cavelti-Weder C.** Targeting colonic macrophages improves glycemic control in high-fat diet-induced obesity. *Commun Biol* 5: 370, 2022. doi:10.1038/s42003-022-03305-z.
28. **Delgado ME**, **Brunner T.** The many faces of tumor necrosis factor signaling in the intestinal epithelium. *Genes Immun* 20: 609–626, 2019. doi:10.1038/s41435-019-0057-0.
29. **Leppkes M**, **Roulis M**, **Neurath MF**, **Kollias G**, **Becker C.** Pleiotropic functions of TNF-α in the regulation of the intestinal epithelial response to inflammation. *Int Immunol* 26: 509–515, 2014. doi:10.1093/intimm/dxu051.
30. **Parameswaran N**, **Patial S.** Tumor necrosis factor-α signaling in macrophages. *Crit Rev Eukaryot Gene Expr* 20: 87–103, 2010. doi:10.1615/critreveukargeneexpr.v20.i2.10.
31. **Varol C**, **Vallon-Eberhard A**, **Elinav E**, **Aychek T**, **Shapira Y**, **Luche H**, **Fehling HJ**, **Hardt WD**, **Shakhar G**, **Jung S.** Intestinal lamina propria dendritic cell subsets have different origin and functions. *Immunity* 31: 502–512, 2009. doi:10.1016/j.immuni.2009.06.025.
32. **Laroui H**, **Viennois E**, **Xiao B**, **Canup BS**, **Geem D**, **Denning TL**, **Merlin D.** Fab'-bearing siRNA TNFα-loaded nanoparticles targeted to colonic macrophages offer an effective therapy for experimental colitis. *J Control Release* 186: 41–53, 2014. doi:10.1016/j.jconrel.2014.04.046.
33. **Kamada N**, **Hisamatsu T**, **Okamoto S**, **Chinen H**, **Kobayashi T**, **Sato T**, **Sakuraba A**, **Kitazume MT**, **Sugita A**, **Koganei K**, **Akagawa KS**, **Hibi T.** Unique CD14 intestinal macrophages contribute to the pathogenesis of Crohn disease via IL-23/IFN-gamma axis. *J Clin Invest* 118: 2269–2280, 2008. doi:10.1172/JCI34610.
34. **Lissner D**, **Schumann M**, **Batra A**, **Kredel LI**, **Kühl AA**, **Erben U**, **May C**, **Schulzke JD**, **Siegmund B.** Monocyte and M1 macrophage-induced barrier defect contributes to chronic intestinal inflammation in IBD. *Inflamm Bowel Dis* 21: 1297–1305, 2015. doi:10.1097/MIB.0000000000000384.
35. **Liu Z**, **Brooks RS**, **Ciappio ED**, **Kim SJ**, **Crott JW**, **Bennett G**, **Greenberg AS**, **Mason JB.** Diet-induced obesity elevates colonic TNF-α in mice and is accompanied by an activation of Wnt signaling: a mechanism for obesity-associated colorectal cancer. *J Nutr Biochem* 23: 1207–1213, 2012. doi:10.1016/j.jnutbio.2011.07.002.
36. **Ding S**, **Chi MM**, **Scull BP**, **Rigby R**, **Schwerbrock NM**, **Magness S**, **Jobin C**, **Lund PK.** High-fat diet: bacteria interactions promote intestinal inflammation which precedes and correlates with obesity and insulin resistance in mouse. *PLoS One* 5: e12191, 2010. doi:10.1371/journal.pone.0012191.
37. **Lam YY**, **Ha CW**, **Campbell CR**, **Mitchell AJ**, **Dinudom A**, **Oscarsson J**, **Cook DI**, **Hunt NH**, **Caterson ID**, **Holmes AJ**, **Storlien LH.** Increased gut permeability and microbiota change associate with mesenteric fat inflammation and metabolic dysfunction in diet-induced obese mice. *PLoS One* 7: e34233, 2012. doi:10.1371/journal.pone.0034233.
38. **Robertson SJ**, **Lemire P**, **Maughan H**, **Goethel A**, **Turpin W**, **Bedrani L**, **Guttman DS**, **Croitoru K**, **Girardin SE**, **Philpott DJ.** Comparison of co-housing and littermate methods for microbiota standardization in mouse models. *Cell Rep* 27: 1910–1919.e2, 2019. doi:10.1016/j.celrep.2019.04.023.
39. **Pinier M**, **Fuhrmann G**, **Galipeau HJ**, **Rivard N**, **Murray JA**, **David CS**, **Drasarova H**, **Tuckova L**, **Leroux JC**, **Verdu EF.** The copolymer P(HEMA-co-SS) binds gluten and reduces immune response in gluten-sensitized mice and human tissues. *Gastroenterology* 142: 316–325e1-12, 2012. doi:10.1053/j.gastro.2011.10.038.
40. **Silva MA**, **Jury J**, **Sanz Y**, **Wiepjes M**, **Huang X**, **Murray JA**, **David CS**, **Fasano A**, **Verdú EF.** Increased bacterial translocation in gluten-sensitive mice is independent of small intestinal paracellular permeability defect. *Dig Dis Sci* 57: 38–47, 2012. doi:10.1007/s10620-011-1847-z.
41. **Sun CM**, **Hall JA**, **Blank RB**, **Bouladoux N**, **Oukka M**, **Mora JR**, **Belkaid Y.** Small intestine lamina propria dendritic cells promote de novo generation of Foxp3 T reg cells via retinoic acid. *J Exp Med* 204: 1775–1785, 2007. doi:10.1084/jem.20070602.
42. **Yan Y**, **Kolachala V**, **Dalmasso G**, **Nguyen H**, **Laroui H**, **Sitaraman SV**, **Merlin D.** Temporal and spatial analysis of clinical and molecular parameters in dextran sodium sulfate induced colitis. *PloS one* 4: e6073, 2009. doi:10.1371/journal.pone.0006073.
43. **de Wit NJ**, **Bosch-Vermeulen H**, **de Groot PJ**, **Hooiveld GJ**, **Bromhaar MM**, **Jansen J**, **Müller M**, **van der Meer R.** The role of the small intestine in the development of dietary fat-induced obesity and insulin resistance in C57BL/6J mice. *BMC Med Genomics* 1: 14, 2008. doi:10.1186/1755-8794-1-14.
44. **Navarrete J**, **Vásquez B**, **Del Sol M.** Morphoquantitative analysis of the Ileum of C57BL/6 mice (Mus musculus) fed with a high-fat diet. *Int J Clin Exp Pathol* 8: 14649–14657, 2015.
45. **Clarke LL.** A guide to Ussing chamber studies of mouse intestine. *Am J Physiol Gastrointest Liver Physiol* 296: G1151–G1166, 2009. doi:10.1152/ajpgi.90649.2008.
46. **Thomson A**, **Smart K**, **Somerville MS**, **Lauder SN**, **Appanna G**, **Horwood J**, **Sunder Raj L**, **Srivastava B**, **Durai D**, **Scurr MJ**, **Keita ÅV**, **Gallimore AM**, **Godkin A.** The Ussing chamber system for measuring intestinal permeability in health and disease. *BMC Gastroenterol* 19: 98, 2019.
47. **Bain CC**, **Bravo-Blas A**, **Scott CL**, **Perdiguero EG**, **Geissmann F**, **Henri S**, **Malissen B**, **Osborne LC**, **Artis D**, **Mowat AM.** Constant replenishment from circulating monocytes maintains the macrophage pool in the intestine of adult mice. *Nat Immunol* 15: 929–937, 2014. [Erratum in *Nat Immunol* 15: 1090, 2014]. doi:10.1038/ni.2967.
48. **Shouval DS**, **Biswas A**, **Goettel JA**, **McCann K**, **Conaway E**, **Redhu NS**, **Mascanfroni ID**, **Al Adham Z**, **Lavoie S**, **Ibourk M**, **Nguyen DD**, **Samsom JN**, **Escher JC**, **Somech R**, **Weiss B**, **Beier R**, **Conklin LS**, **Ebens CL**, **Santos FG**, **Ferreira AR**, **Sherlock M**, **Bhan AK**, **Müller W**, **Mora JR**, **Quintana FJ**, **Klein C**, **Muise AM**, **Horwitz BH**, **Snapper SB.** Interleukin-10 receptor signaling in innate immune cells regulates mucosal immune tolerance and anti-inflammatory macrophage function. *Immunity* 40: 706–719, 2014. doi:10.1016/j.immuni.2014.03.011.
49. **Morhardt TL**, **Hayashi A**, **Ochi T**, **Quirós M**, **Kitamoto S**, **Nagao-Kitamoto H**, **Kuffa P**, **Atarashi K**, **Honda K**, **Kao JY**, **Nusrat A**, **Kamada N.** IL-10 produced by macrophages regulates epithelial integrity in the small intestine. *Sci Rep* 9: 1223, 2019. doi:10.1038/s41598-018-38125-x.
50. **Rivollier A**, **He J**, **Kole A**, **Valatas V**, **Kelsall BL.** Inflammation switches the differentiation program of Ly6Chi monocytes from anti-inflammatory macrophages to inflammatory dendritic cells in the colon. *J Exp Med* 209: 139–155, 2012. doi:10.1084/jem.20101387.
51. **Shi C**, **Pamer EG.** Monocyte recruitment during infection and inflammation. *Nat Rev Immunol* 11: 762–774, 2011. doi:10.1038/nri3070.
52. **Tamoutounour S**, **Henri S**, **Lelouard H**, **de Bovis B**, **de Haar C**, **van der Woude CJ**, **Woltman AM**, **Reyal Y**, **Bonnet D**, **Sichien D**, **Bain CC**, **Mowat AM**, **Reis e Sousa C**, **Poulin LF**, **Malissen B**, **Guilliams M.** CD64 distinguishes macrophages from dendritic cells in the gut and reveals the Th1-inducing role of mesenteric lymph node macrophages during colitis. *Eur J Immunol* 42: 3150–3166, 2012. doi:10.1002/eji.201242847.
53. **Han C**, **Jin J**, **Xu S**, **Liu H**, **Li N**, **Cao X.** Integrin CD11b negatively regulates TLR-triggered inflammatory responses by activating Syk and promoting degradation of MyD88 and TRIF via Cbl-b. *Nat Immunol* 11: 734–742, 2010. doi:10.1038/ni.1908.
54. **Freeman GJ**, **Casasnovas JM**, **Umetsu DT**, **DeKruyff RH.** TIM genes: a family of cell surface phosphatidylserine receptors that regulate innate and adaptive immunity. *Immunol Rev* 235: 172–189, 2010. doi:10.1111/j.0105-2896.2010.00903.x.
55. **Reith W**, **LeibundGut-Landmann S**, **Waldburger J-M.** Regulation of MHC class II gene expression by the class II transactivator. *Nat Rev Immunol* 5: 793–806, 2005. doi:10.1038/nri1708.
56. **Guilliams M**, **Thierry GR**, **Bonnardel J**, **Bajenoff M.** Establishment and maintenance of the macrophage niche. *Immunity* 52: 434–451, 2020. doi:10.1016/j.immuni.2020.02.015.
57. **Grainger JR**, **Konkel JE**, **Zangerle-Murray T**, **Shaw TN.** Macrophages in gastrointestinal homeostasis and inflammation. *Pflugers Arch* 469: 527–539, 2017. doi:10.1007/s00424-017-1958-2.
58. **Monteiro-Sepulveda M**, **Touch S**, **Mendes-Sá C**, **André S**, **Poitou C**, **Allatif O**, **Cotillard A**, **Fohrer-Ting H**, **Hubert E-L**, **Remark R**, **Genser L**, **Tordjman J**, **Garbin K**, **Osinski C**, **Sautès-Fridman C**, **Leturque A**, **Clément K**, **Brot-Laroche E.** Jejunal T cell inflammation in human

obesity correlates with decreased enterocyte insulin signaling. *Cell Metab* 22: 113–124, 2015. doi:10.1016/j.cmet.2015.05.020.

59. **Rohm TV**, **Fuchs R**, **Müller RL**, **Keller L**, **Baumann Z**, **Bosch AJT**, **Schneider R**, **Labes D**, **Langer I**, **Pilz JB**, **Niess JH**, **Delko T**, **Hruz P**, **Cavelti-Weder C.** Obesity in humans is characterized by gut inflammation as shown by pro-inflammatory intestinal macrophage accumulation. *Front Immunol* 12: 668654, 2021. doi:10.3389/fimmu.2021.668654.
60. **Weisberg SP**, **Hunter D**, **Huber R**, **Lemieux J**, **Slaymaker S**, **Vaddi K**, **Charo I**, **Leibel RL**, **Ferrante AW Jr.** CCR2 modulates inflammatory and metabolic effects of high-fat feeding. *J Clin Invest* 116: 115–124, 2006. [Erratum in *J Clin Invest* 116: 1457, 2006]. doi:10.1172/JCI24335.
61. **Luck H**, **Tsai S**, **Chung J**, **Clemente-Casares X**, **Ghazarian M**, **Revelo XS**, **Lei H**, **Luk CT**, **Shi S Y**, **Surendra A**, **Copeland JK**, **Ahn J**, **Prescott D**, **Rasmussen BA**, **Chng MH**, **Engleman EG**, **Girardin SE**, **Lam TK**, **Croitoru K**, **Dunn S**, **Philpott DJ**, **Guttman DS**, **Woo M**, **Winer S**, **Winer DA.** Regulation of obesity-related insulin resistance with gut anti-inflammatory agents. *Cell Metab* 21: 527–542, 2015. doi:10.1016/j.cmet.2015.03.001.
62. **Muller PA**, **Matheis F**, **Mucida D.** Gut macrophages: key players in intestinal immunity and tissue physiology. *Curr Opin Immunol* 62: 54–61, 2020. doi:10.1016/j.coi.2019.11.011.
63. **Greenwood-Van Meerveld B**, **Johnson AC**, **Grundy D.** Gastrointestinal physiology and function. *Handb Exp Pharmacol* 239: 1–16, 2017. doi:10.1007/164_2016_118.
64. **Mah AT**, **Van Landeghem L**, **Gavin HE**, **Magness ST**, **Lund PK.** Impact of diet-induced obesity on intestinal stem cells: hyperproliferation but impaired intrinsic function that requires insulin/IGF1. *Endocrinology* 155: 3302–3314, 2014. doi:10.1210/en.2014-1112.
65. **Mouries J**, **Brescia P**, **Silvestri A**, **Spadoni I**, **Sorribas M**, **Wiest R**, **Mileti E**, **Galbiati M**, **Invernizzi P**, **Adorini L**, **Penna G**, **Rescigno M.** Microbiota-driven gut vascular barrier disruption is a prerequisite for non-alcoholic steatohepatitis development. *J Hepatol* 71: 1216–1228, 2019. doi:10.1016/j.jhep.2019.08.005.
66. **Stenkamp-Strahm C**, **Patterson S**, **Boren J**, **Gericke M**, **Balemba O.** High-fat diet and age-dependent effects on enteric glial cell populations of mouse small intestine. *Auton Neurosci* 177: 199–210, 2013. doi:10.1016/j.autneu.2013.04.014.
67. **Mushref MA**, **Srinivasan S.** Effect of high fat-diet and obesity on gastrointestinal motility. *Ann Transl Med* 1: 14, 2013. doi:10.3978/j.issn.2305-5839.2012.11.01.
68. **Honda M**, **Surewaard BG**, **Watanabe M**, **Hedrick CC**, **Lee W-Y**, **Brown K**, **McCoy KD**, **Kubes P.** Perivascular localization of macrophages in the intestinal mucosa is regulated by Nr4a1 and the microbiome. *Nat Commun* 11: 1329, 2020. doi:10.1038/s41467-020-15068-4.
69. **Muller PA**, **Koscsó B**, **Rajani GM**, **Stevanovic K**, **Berres ML**, **Hashimoto D**, **Mortha A**, **Leboeuf M**, **Li XM**, **Mucida D**, **Stanley ER**, **Dahan S**, **Margolis KG**, **Gershon MD**, **Merad M**, **Bogunovic M.** Crosstalk between muscularis macrophages and enteric neurons regulates gastrointestinal motility. *Cell* 158: 1210, 2014. doi:10.1016/j.cell.2014.08.002.
70. **Kaya B**, **Doñas C**, **Wuggenig P**, **Diaz OE**, **Morales RA**, **Melhem H**, **Hernández PP**, **Kaymak T**, **Das S**, **Hruz P**, **Franc Y**, **Geier F**, **Ayata CK**, **Villablanca EJ**, **Niess JH.** Lysophosphatidic acid-mediated GPR35 signaling in CX3CR1^{+} macrophages regulates intestinal homeostasis. *Cell Rep* 32: 107979, 2020. doi:10.1016/j.celrep.2020.107979.
71. **Caprara G**, **Allavena P**, **Erreni M.** Intestinal macrophages at the crossroad between diet, inflammation, and cancer. *Int J Mol Sci* 21: 4825, 2020. doi:10.3390/ijms21144825.
72. **Li H**, **Xiao Y**, **Tang L**, **Zhong F**, **Huang G**, **Xu JM**, **Xu AM**, **Dai RP**, **Zhou ZG.** Adipocyte fatty acid-binding protein promotes palmitate-induced mitochondrial dysfunction and apoptosis in macrophages. *Front Immunol* 9: 81, 2018. doi:10.3389/fimmu.2018.00081.
73. **Martins de Lima T**, **Cury-Boaventura MF**, **Giannocco G**, **Nunes MT**, **Curi R.** Comparative toxicity of fatty acids on a macrophage cell line (J774). *Clin Sci (Lond)* 111: 307–317, 2006. doi:10.1042/CS20060064.
74. **Kim I-W**, **Myung S-J**, **Do MY**, **Ryu Y-M**, **Kim MJ**, **Do E-J**, **Park S**, **Yoon SM**, **Ye BD**, **Byeon J-S**, **Yang S-K**, **Kim J-H.** Western-style diets induce macrophage infiltration and contribute to colitis-associated carcinogenesis. *J Gastroenterol Hepatol* 25: 1785–1794, 2010. doi:10.1111/j.1440-1746.2010.06332.x.
75. **Gruber L**, **Kisling S**, **Lichti P**, **Martin FP**, **May S**, **Klingenspor M**, **Lichtenegger M**, **Rychlik M**, **Haller D.** High fat diet accelerates pathogenesis of murine Crohn's disease-like ileitis independently of obesity. *PLoS One* 8: e71661, 2013. doi:10.1371/journal.pone.0071661.
76. **Walrath T**, **Dyamenahalli KU**, **Hulsebus HJ**, **McCullough RL**, **Idrovo JP**, **Boe DM**, **McMahan RH**, **Kovacs EJ.** Age-related changes in intestinal immunity and the microbiome. *J Leukoc Biol* 109: 1045–1061, 2021. doi:10.1002/JLB.3RI0620-405RR.
77. **Bujko A**, **Atlasy N**, **Landsverk OJB**, **Richter L**, **Yaqub S**, **Horneland R**, **Øyen O**, **Aandahl EM**, **Aabakken L**, **Stunnenberg HG**, **Bækkevold ES**, **Jahnsen FL.** Transcriptional and functional profiling defines human small intestinal macrophage subsets. *J Exp Med* 215: 441–458, 2018. doi:10.1084/jem.20170057.
78. **Bernardo D**, **Marin AC**, **Fernández-Tomé S**, **Montalban-Arques A**, **Carrasco A**, **Tristán E**, **Ortega-Moreno L**, **Mora-Gutiérrez I**, **Díaz-Guerra A**, **Caminero-Fernández R**, **Miranda P**, **Casals F**, **Caldas M**, **Jiménez M**, **Casabona S**, **De la Morena F**, **Esteve M**, **Santander C**, **Chaparro M**, **Gisbert JP.** Human intestinal pro-inflammatory CD11c^{high} CCR2^{+} CX3CR1^{+} macrophages, but not their tolerogenic CD11c^{-} CCR2^{-} CX3CR1^{-} counterparts, are expanded in inflammatory bowel disease. *Mucosal Immunol* 11: 1114–1126, 2018. doi:10.1038/s41385-018-0030-7.
79. **Wright PB**, **McDonald E**, **Bravo-Blas A**, **Baer HM**, **Heawood A**, **Bain CC**, **Mowat AM**, **Clay SL**, **Robertson EV**, **Morton F**, **Nijjar JS**, **Ijaz UZ**, **Milling SWF**, **Gaya DR.** The mannose receptor (CD206) identifies a population of colonic macrophages in health and inflammatory bowel disease. *Sci Rep* 11: 19616, 2021. doi:10.1038/s41598-021-98611-7.
80. **Hammond KA.** Adaptation of the maternal intestine during lactation. *J Mammary Gland Biol Neoplasia* 2: 243–252, 1997. doi:10.1023/a:1026332304435.
81. **DeJong EN**, **Surette MG**, **Bowdish DME.** The gut microbiota and unhealthy aging: disentangling cause from consequence. *Cell Host Microbe* 28: 180–189, 2020. doi:10.1016/j.chom.2020.07.013.
82. **Eckmann L**, **Kagnoff MF.** Intestinal mucosal responses to microbial infection. *Springer Semin Immunopathol* 27: 181–196, 2005. doi:10.1007/s00281-005-0207-5.
83. **Nguyen HD**, **Aljamaei HM**, **Stadnyk AW.** The Production and Function of Endogenous Interleukin-10 in Intestinal Epithelial Cells and Gut Homeostasis. *Cell Mol Gastroenterol Hepatol* 12: 1343–1352, 2021. doi:10.1016/j.jcmgh.2021.07.005.
84. **Devkota S**, **Wang Y**, **Musch MW**, **Leone V**, **Fehlner-Peach H**, **Nadimpalli A**, **Antonopoulos DA**, **Jabri B**, **Chang EB.** Dietary-fat-induced taurocholic acid promotes pathobiont expansion and colitis in Il10-/- mice. *Nature* 487: 104–108, 2012. doi:10.1038/nature11225.
85. **Kowalski GM**, **Nicholls HT**, **Risis S**, **Watson NK**, **Kanellakis P**, **Bruce CR**, **Bobik A**, **Lancaster GI**, **Febbraio MA.** Deficiency of haematopoietic-cell-derived IL-10 does not exacerbate high-fat-diet-induced inflammation or insulin resistance in mice. *Diabetologia* 54: 888–899, 2011. doi:10.1007/s00125-010-2020-5.
86. **Noti M**, **Corazza N**, **Mueller C**, **Berger B**, **Brunner T.** TNF suppresses acute intestinal inflammation by inducing local glucocorticoid synthesis. *J Exp Med* 207: 1057–1066, 2010. doi:10.1084/jem.20090849.
87. **Kojouharoff G**, **Hans W**, **Obermeier F**, **Männel DN**, **Andus T**, **Schölmerich J**, **Gross V**, **Falk W.** Neutralization of tumour necrosis factor (TNF) but not of IL-1 reduces inflammation in chronic dextran sulphate sodium-induced colitis in mice. *Clin Exp Immunol* 107: 353–358, 2003. doi:10.1111/j.1365-2249.1997.291-ce1184.x.
88. **Naito Y**, **Takagi T**, **Handa O**, **Ishikawa T**, **Nakagawa S**, **Yamaguchi T**, **Yoshida N**, **Minami M**, **Kita M**, **Imanishi J**, **Yoshikawa T.** Enhanced intestinal inflammation induced by dextran sulfate sodium in tumor necrosis factor-alpha deficient mice. *J Gastroenterol Hepatol* 18: 560–569, 2003. doi:10.1046/j.1440-1746.2003.03034.x.
89. **Fine S**, **Papamichael K**, **Cheifetz AS.** Etiology and management of lack or loss of response to anti-tumor necrosis factor therapy in patients with inflammatory bowel disease. *Gastroenterol Hepatol (N Y)* 15: 656–665, 2019.
90. **Aladhami AK**, **Unger CA**, **Ennis SL**, **Altomare D**, **Ji H**, **Hope MC 3rd**, **Velázquez KT**, **Enos RT.** Macrophage tumor necrosis factor-alpha deletion does not protect against obesity-associated metabolic dysfunction. *FASEB J* 35: e21665, 2021. doi:10.1096/fj.202100543RR.
91. **Taeye BMD**, **Novitskaya T**, **McGuinness OP**, **Gleaves L**, **Medda M**, **Covington JW**, **DE V.** Macrophage TNF-α contributes to insulin

resistance and hepatic steatosis in diet-induced obesity. *Am J Physiol Endocrinol Physiol* 293: E713–E725, 2007. doi:10.1152/ajpendo.00194.2007.

92. **Tramunt B**, **Smati S**, **Grandgeorge N**, **Lenfant F**, **Arnal JF**, **Montagner A**, **Gourdy P.** Sex differences in metabolic regulation and diabetes susceptibility. *Diabetologia* 63: 453–461, 2020. doi:10.1007/s00125-019-05040-3.
93. **Breznik JA**, **Schulz C**, **Ma J**, **Sloboda DM**, **Bowdish DME.** Biological sex, not reproductive cycle, influences peripheral blood immune cell prevalence in mice. *J Physiol* 599: 2169–2195, 2021. doi:10.1113/JP280637.
94. **Bain CC**, **Hawley CA**, **Garner H**, **Scott CL**, **Schridde A**, **Steers NJ**, **Mack M**, **Joshi A**, **Guilliams M**, **Mowat AMI**, **Geissmann F**, **Jenkins SJ.** Long-lived self-renewing bone marrow-derived macrophages displace embryo-derived cells to inhabit adult serous cavities. *Nat Commun* 7: ncomms11852, 2016. doi:10.1038/ncomms11852.
95. **Verdú EF**, **Deng Y**, **Bercik P**, **Collins SM.** Modulatory effects of estrogen in two murine models of experimental colitis. *Am J Physiol Gastrointest Liver Physiol* 283: G27–G36, 2002. doi:10.1152/ajpgi.00460.2001.
96. **Bábíčková J**, **Tóthová Lõ**, **Lengyelová E**, **Bartonõová A**, **Hodosy J**, **Gardlík R**, **Celec P.** Sex differences in experimentally induced colitis in mice: a role for estrogens. *Inflammation* 38: 1996–2006, 2015. doi:10.1007/s10753-015-0180-7.
97. **Hases L**, **Archer A**, **Indukuri R**, **Birgersson M**, **Savva C**, **Korach-André M**, **Williams C.** High-fat diet and estrogen impacts the colon and its transcriptome in a sex-dependent manner. *Sci Rep* 10: 16160, 2020. doi:10.1038/s41598-020-73166-1.